A MODEL FOR BLOOD COAGULATION AND LYSIS UTILIZING THE INTRINSIC AND EXTRINSIC PATHWAYS

A Dissertation

by

DANIEL EDWARD LACROIX

Submitted to the Office of Graduate Studies of
Texas A&M University
in partial fulfillment of the requirements for the degree of

DOCTOR OF PHILOSOPHY

May 2011

Major Subject: Mechanical Engineering

A MODEL FOR BLOOD COAGULATION AND LYSIS UTILIZING THE INTRINSIC AND EXTRINSIC PATHWAYS

A Dissertation

by

DANIEL EDWARD LACROIX

Submitted to the Office of Graduate Studies of
Texas A&M University
in partial fulfillment of the requirements for the degree of

DOCTOR OF PHILOSOPHY

Approved by:

Chair of Committee,	Kumbakonam Rajagopal
Committee Members,	James Moore, Jr.
	Kalyana Nakshatrala
	Duncan Maitland
Head of Department,	Dennis O'Neal

May 2011

Major Subject: Mechanical Engineering

ABSTRACT

A Model for Blood Coagulation and Lysis Utilizing the Intrinsic and Extrinsic Pathways.

(May 2011)

Daniel Edward LaCroix, B.S., Trinity University;

M.S. Texas A&M University

Chair of Advisory Committee: Dr. Kumbakonam Rajagopal

Blood is a complex mixture of formed cellular elements, proteins, and ions dissolved in a solution. It is a difficult fluid to model because it is a shear-thinning, viscoelastic fluid that stress-relaxes. In this study, a new mathematical model for whole blood is developed from a general equation for a fluid with a shear dependent viscosity. The model is then used as a backdrop for 28 different biochemical factors interacting to form a clot. The full intrinsic and extrinsic pathways are both used in the simulation; the inclusion of the full intrinsic pathway is something that had not been done prior to this work. The model is executed in one spatial direction in an infinite domain as well as within a rigid walled cylinder using a finite volume scheme. The rigid wall, similar to the new mathematical equation for blood, is an oversimplification of actual in-vitro conditions. The results of both simulations show the formation and dissolution of the clot. Sensitivity analysis is then performed in the finite domain model by adjusting the initial levels of factors Va and Xa. The results show that increasing the initial level of one or both of these factors leads to the quicker formation of a clot.

DEDICATION

To my mother, a mighty force.

ACKNOWLEDGEMENTS

There are many I would like to acknowledge during the course of my dissertation work. Dr. Rajagopal has been an inspiration and of tremendous assistance. Though many are familiar with his vast intelligence, I have come to know him through his sense of humor and clever wit. It is an aspect of our relationship that I value. He has pushed me and expanded my knowledge base in fantastic ways; truly, an amazing mentor.

The rest of my committee has been exactly as I hoped they would be: challenging me to do better and helpful along the way. Drs. Maitland, Nakshatrala, and Moore have all been excellent committee members.

My family and friends who have supported me are beyond description. They keep me humble, are incredibly supportive, and they have looked forward to my obtaining my Ph.D. almost as much as I do. They have all been wonderful along each step of this long journey.

Thank you to my lab mates, Satish, Shriram, Gupta, Atul, Saradhi, and Vit, for camaraderie and lively discussions about all manner of topics. I enjoy them all. A special thank you to Lubos Pirkl, whose programming knowledge propelled me forward.

TABLE OF CONTENTS

Page

LIST OF FIGURES

Page

LIST OF TABLES

INTRODUCTION

Blood is a liquid that circulates in the body and is one of the principal components of the cardiovascular system. The cardiovascular system is responsible for the delivery and removal of nutrients, gases, and necessary components throughout the body. It is made up of the heart, which acts as a pump, as well as the arteries, arterioles, capillaries, venules, and veins that carry and distribute blood throughout the body. Blood is comprised of formed cellular elements and proteins suspended in an aqueous solution. The formed cellular elements include erythrocytes (or red blood cells), leukocytes (or white blood cells), and platelets. The aqueous solution is plasma and consists of mostly water as well as dissolved proteins (such as fibrinogen and prothrombin) and ions (such as Ca^{+}, HCO_3^{-}, etc.).

Blood Distribution

Blood is pumped throughout the body by the heart. A large and complicated network of blood vessels is used to distribute blood. The blood vessels range in diameter from 2.5 cm (the aorta) to 8 μm (capillaries) (Martini et al., 2001). The pathways leading away from the heart are called arteries while those that usher blood on its return to the heart are called veins. The vessels are lined with endothelium which functions to allow secretion and absorption as well as protection. A healthy endothelium will actively suppress unnecessary clot formation, vascular inflammation, as well as hypertrophy (Landmesser et al., 2004).

This dissertation follows the style of Journal of Theoretical Biology.

It seems obvious that, without disruption, cardiac output and venous return are equal. Furthermore, within isolated tissues the in-flow and out-flow of blood remain equal. However, this does not mean that blood flows equally in arteries and veins. On the contrary, the two flow quite differently. Arterial blood flows in pulses while venous blood flow is essentially steady. The maximum velocity, average velocity, and pressure are higher in arteries. These flow characteristics are logical when considering the manner in which blood is pumped. Arterial blood is moved by the periodic contraction of the heart, and while outflow from the heart is distinctly pulsatile, in smaller vessels it is much steadier. This is because the larger arteries expand during systole (when the heart contracts), storing blood. During diastole (when the heart fills with blood), the arteries contract, thus giving up the blood that was stored. How much a blood vessel expands and contracts is known as compliance. Venous blood flows smoothly because it deposits into atria of the heart that act as reservoirs before being pumped back into the body (Rajagopal and Lawson, 2007).

Components of Blood

Erythrocytes are actually small hemoglobin solutions bound by a flexible membrane. While in large pathways, red blood cells (or RBCs) are round discs with a diameter of about 7.7 microns and outer edges that are roughly twice as thick as the center (2.8 microns and 1.4 microns respectively) (Rajagopal and Lawson, 2007) . This discrepancy in thickness is important because as the RBCs enter smaller pathways they deform into a parabolic shape. The difference in thickness means that there is less resistance to this deformation. RBCs also contain hemoglobin, which is responsible for

transporting oxygen to the body. In addition to delivering oxygen, RBCs also help deliver carbon dioxide (mostly in the form of bicarbonate) to the lungs. Volumetrically, erythrocytes make up 97% of the formed elements in blood (Anand, et al. 2003). In large arteries, RBCs will bind together to form rouleaux (Chien et al., 1970). The shear thinning qualities of blood can be attributed to the disaggregation of rouleaux that form at low shear and the deformability of RBCs (Chien et al., 1966). Additionally, RBCs stay a minimum distance away from the wall due to the Fahreus-Lindqvist effect (Fåhreus and Lindqvist, 1931).

In addition, recent research by scientists at the National University of Singapore have uncovered another function of erythrocytes: defense. Their findings state that when bacteria breach a red blood cell, a plethora of dangerous chemicals known as free radicals are released. The free radicals latch on to the bacteria and break open the cell wall, effectively killing the bacteria. The free radicals are also harmful to human tissue, but the proximity of the bacteria usually ensures that they will be the target rather than the endothelium. This defense mechanism has been found in horseshoe crabs as well which suggests that it is, evolutionarily speaking, an old defense mechanism (Kesava, 2007).

Leukocytes, or white blood cells (WBC's), are part of the body's immune system, and act as the main aggressors against foreign agents. There are five different kinds of WBC's: neutrophils, eosinophils, and basophils are referred to as granulocytes while lymphocytes and monocytes are called agranular leukocytes. Granulocytes are roughly 8-15 microns across while the agranular leukocytes are much bigger with sizes

between 15 and 25 microns (Rajagopal and Lawson, 2007). Each leukocyte serves a separate purpose.

Neutrophil accumulation is associated with the immune system as well as inflammation and can be seen across a wide array of medical conditions from infection to cancer. The neutrophil combats bacterial infection as well as helping to rid the body of unnecessary (and therefore unwanted) extracellular deposits as well as damaged tissue. As neutrophils begin to fight infection they release granule enzymes, an oxidase, H_2O_2, and several lipids. The granules are mostly composed of two enzymes: the azurophil and the specific. The azurophil seeks out and destroys microbials while the specific replenishes membranes and limits reactions. It is worth noting that this leukocyte's actions also cause inflammation and tissue damage to the body, which is normal for neutrophil accumulation (Baggiolini et al., 1989).

How neutrophils combat microbes is especially interesting. It was previously thought that oxygen and oxygen reactive elements were activated to combat bacteria and fungi. However, this is incorrect. In actuality, electrons are pumped into the phagocytic vacuole (the target fungi or bacteria) which creates a charge difference across the membrane. As ions move across the membrane to rectify the charge difference, a path is created that allows the granule enzymes and superoxide to be released into the vacuole thus killing the target microbe (Segal, 2005).

While similar to neutrophils in their association with the immune system, eosinophils are involved in an extremely wide variety of processes. Within its function as a fighting agent, eosinophils are stimulated by tissue injury, infections, allergens, and

tumor formation. In response to stimulation, four different cytotoxic proteins are released. Eosinophils also discharge a wide array of cytokines responsible for lymphocyte proliferation and activation as well as ongoing communication with the lymphocytes after they have been mobilized (Rothenberg and Hogan, 2006).

Basophils are the least common WBC's compromising less than 1% of leukocytes and have often been considered to be at best, minor and at worst, redundant. There exist cells in tissue that behave and perform nearly identical to basophils that are called mast cells (Sharon, 1998). Recent research done on mice with depleted basophils showed no significant effects on classic allergic reactions. In fact, it prevented the development of immunoglobin-E mediated chronic allergic dermatitis that is associated with eosinophil infiltration. Thus, basophils play an important role in the development of immunoglobin-E mediated chronic allergic inflammation as an initiator rather than in response to other immune system responses (Obata et al., 2007). Though they make up a small portion of WBCs, they are able to recruit assistance and call specific situations to the attention of the more capable elements of the immune system. This may be the reason that there are such low numbers of basophils found within blood: they are merely intended to alert more capable leukocytes as well as act as reinforcements to the battle being waged by mast cells.

Lymphocytes can be broken down into three groups: T-cells, B-cells, and natural killer (NK) cells. Research into these elements yields a veritable library of information that delves deep into specifics surrounding their origin, role within the immune system, and relationship with elements that are outside the scope of this paper. As is, a general

overview of each cell and its variations will be discussed.

T-cells are so named because they are formed primarily in the Thymus. All T-cells have several receptors on their membrane referred to as T-cell receptors. The receptors may be comprised of an α-β chain or a δ-γ chain, but not both. A T-cell only contains one type of receptor that is repeated. Within humans, α-β cells make up between 85 and 95% of all T-cells. There are three main types of T-cells; T-cytotoxic, T-helper, and T-suppressor, and each serves a different purpose within their function as a T-cell. T- cytotoxic cells are sometimes called effectors because they effectively kill target cells. In order to do this, the T-cytotoxic cell bonds to the MHC class I complex of a cell with an unrecognizable antigenic determinant. T-helper cells, as their name implies, encourage the immune system response. T-suppressor cells do the opposite and work to dampen the immune system response. Both T-helper and T-suppressor work through direct contact with other cells as well as by the secretion of soluble molecules that impact the function of other cells (Sharon, 1998).

B-cells perform a similar function as T-cells, but in a different way. The B-cell antibody is shaped like a “Y”. The branches at the top are known as the Fab region, and provide two sites to bind antigens. The base part of the “Y” is referred to as the Fc region and is responsible for effector and transport functions. It doesn’t destroy the antigen itself, but rather clings to the target cell and rallies other soluble proteins as well as specific effector cells to its position. As such, B-cells often become the targets of T-cells. Both T-cells and B-cells develop memories to specific antigens. The result is that in addition to the primary immune system response, there is also a bigger and faster

(thus better) secondary antibody response. The combination of the B- and T-cell memory often means that re-exposure to a pathogen will not result in disease (Sharon, 1998). This is mostly likely the main reason that seasonal ailments are only contracted once.

Natural Killer cells derive their name from their ability to kill host cells. NK-cells are similar to B-cells and especially similar to T-cells, but lack a receptor mechanism similar to either. In addition, on the average, NK-cells are slightly larger than the other two types of lymphocytes (9-15 micrometers opposed to 6- 15 micrometers respectively). An NK-cell has two receptors that, in effect, serve as the conscious of the cell. The activation receptor binds to ligands of a potential target and triggers the killing. The inhibitory receptor binds to the MHC class I molecules and, if engaged, transmits a protective signal that blocks the activation, thus preserving the target cell from destruction. Some pathogens may decrease the MHC class I expression in host cells as an effective way to avoid targeting by T-cytotoxic cells, but this results in targeting by NK-cells (Sharon, 1998). As the example shows, it is important to have more than one way to dispose of foreign cells. As an antigen adjusts to be more resistant to one lymphocyte, it often becomes more vulnerable to another.

The platelet is the final cellular element of blood to be discussed. Platelets are made in bone marrow, and their levels in blood are monitored and determined by the spleen. The average life span of a platelet is seven to ten days, and under steady state conditions, roughly two thirds of that will be spent in circulation and the other third will be spent in the spleen (Rajagopal and Lawson, 2007). The main function of platelets is to repair severed blood vessels. With regards to distribution, platelets drift towards the

wall; thus, they are not evenly dispersed throughout a blood vessel radially (Eckstein and Belgacem, 1991).

The cellular matter discussed to this point accounts for roughly 44% of whole blood; plasma accounts for the remaining 56%. The majority of plasma is water, which makes up 92-93%. The remaining 7-8% is a myriad of proteins and various ions (Anand et al., 2003). Among these are the factors critical in the formation of a clot, including but not limited to the inactivated and activated forms of factors V, VII, VIII, IX, X, XI, XII, as well as those that work against clotting such as Protein C, Tissue Factor Pathway Inhibitor, and Anti-thrombin III.

In mechanical terms, blood is a difficult fluid to model. It is primarily made up of plasma, a newtonian fluid, however, the work of Chien et al. (1966) shows that blood is shear-thinning. This description also doesn't encompass the full complexity of blood. Thurston (1972) showed that not only is blood viscoelastic, but that it also stress-relaxes.

Blood Coagulation

During times of vascular damage, a clot is formed in a process known as thrombosis to prevent blood loss. Blood coagulation is an involved combination of positive and negative feedback mechanisms. During normal flow, the negative feedback factors dominate to halt the unnecessary formation of blood clots. When the blood vessel wall (or endothelium) is ruptured, it triggers three pathways, often referred to as Virchow's Triad (Anand et al., 2003). The first, is initiated by the activation of platelets. The second, the extrinsic pathway, so called because it involves factors not found in whole blood, is initiated by the release of tissue factor (TF) by the subendothelium. The

final pathway is the intrinsic pathway because it is triggered by factors found in whole blood. The final result of thrombosis is a fibrin net or mesh to which platelets adhere, thus forming a thrombotic plug. Two graphic images depicting the extrinsic and intrinsic pathways are presented in Fig. 1 and 2.

The platelet pathway is characterized by the activation of blood platelets. When activated, a platelet changes from a smooth disc into a spindly orb. Platelets can be activated by high shear stress as well as by chemical agonists. After the vessel wall is damaged, platelets attach to von Willebrand factor, collagen, and fibronectin located in the sublayer of the endothelium. As the platelets bond with the von Willebrand factor, they begin to resist the shear stress imparted by the passing blood. Additionally, as the platelet bonds to the collagen of the wall, platelet receptors are activated that initiate thrombaxane A_2 formation as well as the release of storage granules (including ADP). The thrombaxane A_2 and ADP are recognized by receptor sites on passing platelets, which are then activated and change shape to form an aggregate around the established platelets. The granules also cause the release of procoagulant phospholipids to the platelet surface which act to accelerate the thrombus formation by acting as catalysts and speeding up reactions (Rand et al., 2003).

The extrinsic pathway is triggered by the release of tissue-factor (TF) from the subendothelium following rupture of the endothelium. TF binds with factor VIIa to form the TF-VIIa complex, which in turn activates factors IX and X to IXa and Xa, respectively (Anand et al., 2008). The extrinsic pathway is counteracted by tissue factor pathway inhibitor (TFPI) and antithrombin-III (ATIII).

The intrinsic pathway is activated by factor XII (or Hageman factor) coming into contact with a negatively charged surface, such as that found in the subendothelium. For this reaction, high molecular weight kininogen (HMWK) is present as a cofactor. When factor XII is activated, it splits into equal amounts of α-XIIa and β-XIIa (Revak, 1977). These two factors, with independent rate constants, convert pre-kallikrein (preK) to kallikrein (kalli), which serves to activate more factor XII. This positive feedback loop serves as the main form of factor XII activation and greatly increases the amount of factor XIIa being produced (Tankersley and Finlayson, 1984). Factor XIIa activates XI to XIa, and XIa then activates IX to IXa. Protein C1-inhibitor (C1INH) serves to inhibit XIIa, kallikrein, and XIa.

After the intrinsic and extrinsic pathways are initiated, they converge at the activation of factor X. Together, Xa and Va make up the complex prothrombin, which converts II to IIa. As thrombin production continues, it converts fibrinogen (I) to fibrin (Ia). The strands of fibrin bind with platelets as the clot begins to form. As thrombin (and fibrin) production continue, the extravascular space above the damaged endothelium becomes filled. Now fully developed, the clot covers the damaged area and prevents blood from making further contact as well as preventing more pro-coagulant zymogens from reaching the extra-vascular compartment. Within the intravascular compartment, two different mechanisms serve to inhibit enzymes from escaping the clot. The first is Antithrombin III-Heparin Sulfate complex (HS-ATIII), which serves to inactivate IIa, Xa, and IXa. The second is Activated Protein C (APC) which is formed when Protein C binds to thrombin bound to endothelial thrombomodulin. APC

suppresses the formation of thrombin and fibrin by inactivating Va and VIIIa.

The breakdown of the clot, or fibrinolysis, is initiated by the same thrombin that promotes clot development. Thrombin (IIa) as well as fibrin (Ia) induce endothelial cells within the intravascular compartment to release tissue-plasminogen activator (tPA). Plasminogen (PLS) binds with tPA and Ia to form a complex that converts plasminogen to plasmin (PLA), the main degradation agent of fibrin (Ia). As the fibrin mesh breaks down, more binding sites are revealed to convert more PLS to PLA, thus advancing the dissolution of the clot. A higher concentration of PLA will result in a faster rate of degradation. Fibrinolysis is complete when the clot is completely dissolved. Any remaining plasmin is deactivated by α_2-antiplasmin (α_2 AP).

The activations (and subsequent inactivations) presented above can be mathematically modeled in various ways. The first is with Michaelis-Menten kinetics, in which the reaction rate is dependent upon the maximum value of the reaction as well as the amount of substrate available. A reaction following Michaelis-Menten kinetics has the form:

$$\frac{\partial[B]}{\partial t} = \frac{V_{max}[S]}{K_m + [S]} \tag{1}$$

where the change in concentration of some substance B is affected by V_{max}, the maximum rate of the reaction, K_m, the inverse of enzyme availability, and S, the concentration of substrate. A first order reaction has the form:

$$\frac{\partial[B]}{\partial t} = k_1[B] \tag{2}$$

where B represents the concentration of a substance that changes with respect to the

activation (or deactivation) constant and the concentration of *B* present. Here, k_1 has units of s^{-1}. The final mode of activation considered is second order, following:

$$\frac{\partial[B]}{\partial t} = k_2[A][B] \tag{3}$$

For reactions of this form, the rate of change in the concentration of *B* is dependent on the concentrations of both *A* and *B*. For this reaction, k_2 has units of $s^{-1}mol^{-1}$.

Coagulation Disorders

Disorders that arise surrounding the formation of clots are plentiful, and have been linked to a myriad of medical problems including, but not limited to, myocardial infarcation (heart attack), stroke, and ischemia. Pulmonary thromboembolism is an especially grave problem arising from clotting disorders, causing 5-10% of all hospital deaths (Goodnight and Hathaway, 2001). Clotting disorders can be broken into two groups: hemorrhagic and thrombotic. Hemorrhagic disorders are characterized by the body not developing a clot in response to vascular damage. Thrombotic disorders cause the body to form unnecessary clots. An excess or deficiency of a specific factor within the clotting cascade can have adverse effects on thrombosis.

Deep veinous thrombosis (DVT) and pulmonary thromboembolism are two of the major problems that may arise from a hypercoagulable state. DVT is characterized by a clot forming in a deep (or large) vein, thus blocking blood flow to parts of the body. Additionally, the clot could become dislodged, thus causing an embolism. Typically, these two conditions are caused by an excess of clotting factors, clotting factors in a mutant and hyperactive state, an insufficient amount of anti-coagulants, or anti-coagulants in a mutant and ineffective form. The most common forms are Factor V

Leiden, mutant Prothrombin, Protein C deficiency, Protein S deficiency, and ATIII deficiency. Endothelial dysfunction could also be considered a risk. Treatment in most cases is done by administering anticoagulants (Anand et al., 2003).

Individuals with a deficiency of Factor XII do not show abnormal bleeding. However, there is an inverse association between myocardial infarcation and high levels of XII which suggests that there is a protective effect for elevated concentrations. In its activated form, XIIa, heightened levels have been associated with an increased risk for coronary heart disease while low levels pose a risk of coronary artery disease and stroke in middle aged men (Gailani and Renné, 2007).

A deficiency of factor VIII, IX, or XI results in hemorrhagic disorders known haemophilia A, B, and C, respectively. Typically, the factor in question is at a level 70% below normal. Severe cases of haemophilia A and B are associated with hemorrhage into joints and muscles, as well as soft tissue bleeding that can be life threatening. Haemophilia C is usually milder, characterized by trauma or soft tissue related hemorrhage, primarily with tissue that has high fibrinolytic activity (Gailani and Renné, 2007). Typically, the disorder is treated by the intravenous replacement of the deficient factor (Goodnight and Hathaway, 2001).

Elevated levels of factors VIII, IX, and XI can prove to be equally problematic. Studies have shown that individuals with VIII above the upper limit of normal have roughly 5 times the possibility of venous thromboembolism. Similarly, levels of IX and XI in the top 10% have twice the risk of thromboembolism. High levels of factor XI have also been associated with an increased risk of heart attack, stroke, and ischemia

(Gailani and Renné, 2007).

Thrombocytopenia, or low platelet count, is a hemorrhagic disorder. This may be caused by a lack of platelet synthesis, improper regulation by the spleen, or excessive platelet destruction (Anand et al., 2003). The goal of treatment is not to achieve normal levels, but rather to achieve adequate levels; steroids often have a positive response. In adult cases, if all other treatments fail, a spleenectomy may be done (Goodnight and Hathaway, 2001). Platelet dysfunction, though different than thrombocytopenia, may have similar results. The administering of drugs for other afflictions may inactivate thromboxane A2 and/or ADP release. This results in the reduction of platelet adhesion and recruitment (Anand et al., 2003).

Von Willenbrand's disease is a genetic affliction causing a qualitative or quantitative shortfall of von Willenbrand factor (vWF). As has already been discussed, vWF plays an important role in the platelet adhesion to blood vessel walls, but it is also a carrier protein for factor VIII. Von Willenbrand's disease is characterized by mucocutaneous bleeding, and has several variations with varying effects (Goodnight and Hathaway, 2001).

Disseminated Intravascular Coagulation (DIC) is a complex entity that may have many stimuli. It is characterized by early formation of intravascular thrombi followed by subsequent coagulation factor depletion and augmented fibrinolysis; the end result is excessive bleeding. Thus, DIC is both a thrombotic and hemorrhaging disorder. It may be a complication caused by sepsis or trauma. Treatment depends on the stage it is recognized and often attempts to treat the underlying cause. Early thrombotic DIC is

countered by administering anticoagulants to prevent thrombus formation and also prevent coagulation factor depletion. Later stages of DIC, or bleeding DIC, is treated with agents to either augment coagulation or inhibit fibrinolysis (Anand et al., 2003).

The most popular anti-coagulant drugs are Heparin and Warfarin. Heparin works by impairing platelet function and irreversibly inactivating factors IXa, Xa, and XIa, all three of which are found in the intrinsic pathway. Warfarin deactivates factors VII, IX, X, and II, which are found in the intrinsic and extrinsic pathways. In order to effectively model the effects of either of these anticoagulants, the inclusion of the full intrinsic pathway is required.

A complete blood coagulation model would include the full scope of hemodynamics and the three major pathways of coagulation. The model could then be put to use in several capacities. A well-conceived and well executed model could replace experiments as well as simulate potential disturbances to clotting hemodynamics caused by disease or medication. Further, the model could be used in the design of implantable stents, ventricular assist devices, and artificial hearts.

LITERATURE REVIEW

Whole Blood Literature Review

A variety of models for whole blood have been formulated with varying complexity. In 1966, experiments by Chien et al. showed that for whole blood, shear rate and viscosity do not have a linear relationship i.e. whole blood is non-newtonian. Walburn and Schneck (1976) posed a power law model based upon the hematocrit as well as a calculated quantity of fibrinogen and globulins. However, the model shows a decreasing viscosity at higher shear rates when whole blood is considered to behave as a newtonian fluid (Pedley, 1980). A Casson fluid model is presented by Fung (1997) and follows the general shape of experimental data, however it overestimates viscosity at high shear rates (Johnston et al., 2004). In 1991, Cho and Kensey presented a Carreau model that corrected this overestimation and was relatively accurate. Luo and Kuang (1992) presented a three-parameter constitutive equation that was a modification of Casson's equation and is adaptable over a wider range of shear rates. The apparent viscosity for all of these models is presented in Appendix C.

Other models have been put forth more recently. In 1996, Yeleswarupu proposed a generalization of an Oldroyd-B fluid model that fit data better than other models used at the time (Anand and Rajagopal, 2004). However, the model did not have a thermodynamic basis, something that Rajagopal and Srinivasa (2000) corrected. In 2004, Anand and Rajagopal further advanced this model to more accurately fit experimental data. Because the model put forth by Anand and Rajagopal represents the culmination of the Oldroyd-B fluid models, it is also presented in Appendix C.

While the Walburn and Schneck model and Casson model use hematocrit, no other model uses constituents within the blood to adjust the viscosity. Although blood is a mixture of various cells, proteins, ions, glycoproteins, and platelets, all of the models discussed herein model blood as a continuum.

Clotting Model Literature Review

At a similar time, papers authored by MacFarlane (1964) and Davie and Ratnoff (1964) showed the coagulation pathways as enzyme cascades. As a result, mathematical models have emerged to illustrate and predict coagulation processes. The first such model was by Levine (1966) who mathematically characterized general enzyme cascades using the work of MacFarlane (1964) and Wald and Bownds (1965) as guides.

In 1984, Nesheim et al. designed a program to mathematically simulate the functional properties of prothrombin using experimentally determined kinetic parameters. Simulations were carried out for a given set of initial concentrations of reaction components. The distribution of enzymatic components and substrates were then calculated from the distribution, fractional binding, and local and bulk concentrations. The results were then compared with experimental data.

In 1986, Nemerson and Gentry proposed a model showing that the activation of factors IX and X is predicated on their interaction with tissue factor and factor VIIa. Equations were derived to show that product formation is accompanied by the release of the enzyme activator complex. The model was verified by experiments using bovine tissue factor.

Khanin and Semenov (1989) proposed a non-linear model of the activation using

factors VIII, X, V, II, I, and their activated forms. The model is notable because it shows the reciprocal activation of IIa and Va. Deactivations of the factors used were also taken into account. The majority of the activation (and deactivations) were modeled as first order, only IIa was modeled using Michaelis-Menten kinetics.

Jones and Mann (1994) proposed a more involved model showing the full extrinsic pathway to activation utilizing TF, VIIa, IX, IXa, X, Xa, V, Va, II, and IIa. The activation and deactivation kinetics were modeled using first and second order rate constants. The end result is 18 first order differential equations. The thrombin, Xa, and IXa production levels were compared to experimental data. The model stops short of showing fibrin activation and thus clot development. It also neglects to include the inhibiting factors of the extrinsic pathway.

In 1996, Zarnitsina et al. proposed a model that included the formation of fibrin and also incorporated the anticoagulation effects of Activated Protein C (APC). The model incorporates Michaelis-Menten, first order, and second order kinetics to show the interactions of factors IX, IXa, VIII, VIIIa, V, Va, X, Xa, II, IIa, I, Ia, and APC. The end result is a spatial model of eight differential equations and one ordinary differential equation. The model set a boundary condition for factor IXa only. Though the authors call it a model of the intrinsic pathway, the factors most associated with the intrinsic pathway (XII, XIIa, XI, XIa) were not included.

The extrinsic pathway was modeled in more detail by Kuharsky and Fogelson in 2001. Though fibrin is not included, the full extrinsic pathway along with the inhibitors TFPI, APC, and ATIII and platelet interactions are modeled. The model also

incorporates flow and adjusts the flux of components based upon boundary layer thickness. The final model is a system of 59 ordinary differential equations.

Bungay et al. (2003) modeled the extrinsic pathway and its inhibitors in a static fluid environment. The model is significantly different because it differentiates between fluid and lipid bound factors and complexes. Thus, reactions take place between factors and complexes both in the fluid and on the lipid membrane. The result is 73 ordinary differential equations using first and second order kinetics.

Anand et al. (2003) modeled the extrinsic pathway in a generalized oldroyd-B fluid with flow in one spatial direction. The model incorporates Michaelis-Menten as well as first and second order reaction kinetics in 25 coupled convection-diffusion-reaction partial differential equations. It is a two phase model with the clot behaving as fluid with much higher viscosity. Platelets are included in the model as protein binding sites as well as catalytic surfaces. The intrinsic pathway was not included, nor was the fibrinolysis of the clot.

Bodnar and Sequiera (2008) modeled the formation of a clot using only the extrinsic pathway in a medium sized artery. A shear-thinning fluid was used for blood, 23 partial differential equations were used to model the biochemical reactions taking place, and only the growth of the clot was shown. The model oversimplified the level of TF-VIIa in the boundary conditions, failed to show the lysis of the clot, did not include the intrinsic pathway, and used a lower velocity than is found in-vivo for the size of the artery modeled.

The most pertinent work to this study was done by Anand et al. (2008). The

model showed the formation and lysis of a clot using 23 partial differential equations to mimic the full extrinsic pathway. The clot was modeled in one dimensional direction in quiescent plasma over a thrombogenic pane. Thrombin production results compared favorably with experimental data from Butenas et al. (1999). The model was then used to look at Protein C and ATIII deficiencies and their effects on initiation time as well as the size of the clot. The model failed to include the intrinsic pathway.

PRELIMINARIES

This section will discuss a few of the concepts from continuum mechanics that will be used to develop the model.

For a body $\boldsymbol{B}$, let $\kappa_R(\boldsymbol{B})$ be the reference configuration and $\kappa_t(\boldsymbol{B})$ be the current configuration at some time t. Now, a sufficiently smooth motion, $\boldsymbol{\chi}$, may take place. The motion is a one-to-one mapping such that for every point $\boldsymbol{X} \in \kappa_R(\boldsymbol{B})$ there is a point $\boldsymbol{x} \in \kappa_t(\boldsymbol{B})$. Thus,

$$\boldsymbol{x} = \boldsymbol{\chi}(\boldsymbol{X}, t) \quad or \quad \boldsymbol{X} = \boldsymbol{\chi}^{-1}(\boldsymbol{x}, t) \tag{4}$$

Any property of the body, φ, can be expressed as:

$$\varphi = \hat{\varphi}(\boldsymbol{X}, t) = \tilde{\varphi}(\boldsymbol{x}, t) \tag{5}$$

The velocity, $\boldsymbol{v}$, and acceleration, $\boldsymbol{a}$, are defined as:

$$\boldsymbol{v}(\boldsymbol{X}, t) = \frac{\partial \boldsymbol{\chi}}{\partial t} \tag{6}$$

$$\boldsymbol{a}(\boldsymbol{X}, t) = \frac{\partial^2 \boldsymbol{\chi}}{\partial^2 t} \tag{7}$$

Additionally, the deformation gradient, $\mathbf{F}$, and the Cauchy-Green left and right stretch tensors, respectively are:

$$\mathbf{F} = \frac{\partial \mathbf{x}}{\partial \mathbf{X}} \tag{8}$$

$$\mathbf{B} = \mathbf{F}\mathbf{F}^T \tag{9}$$

$$\mathbf{C} = \mathbf{F}^T\mathbf{F} \tag{10}$$

Now, the velocity gradient, $\mathbf{L}$, can be defined as:

$$\mathbf{L} = \frac{\partial \mathbf{v}}{\partial \mathbf{X}} = grad(\mathbf{v}) \tag{11}$$

The symmetric part of the velocity gradient, **D**, is:

$$\mathbf{D} = \frac{1}{2}\left(\mathbf{L} + \mathbf{L}^T\right) \tag{12}$$

Because blood will be treated as an incompressible fluid, the trace of the symmetric part of the velocity gradient will be zero.

$$tr(\mathbf{D}) = 0 \tag{13}$$

The equation governing the flow and reaction of each of the terms used in the biochemical aspect of the model is:

$$\frac{\partial [C_i]}{\partial t} + div\left([C_i]\mathbf{v}\right) = div\left(D_i \frac{\partial [C_i]}{\partial \mathbf{x}}\right) + G_i; i = 1,...,28 \tag{14}$$

where C_i is the concentration of a specific constituent, D_i is the diffusion term correlating to the constituent, **v** is the velocity field of the fluid (for this work, zero), **x** is the spatial dimension, and G_i is the reaction term responsible for the production or depletion of the constituent in question. Each constituent is assumed to exist at every point and to not affect the overall flow rate.

The balance of mass, linear momentum and angular momentum are defined as:

$$\frac{D\rho}{Dt} + \rho div(\mathbf{v}) = 0 \tag{15}$$

$$div(\mathbf{T}) + \rho\mathbf{b} = \rho\frac{D\mathbf{v}}{Dt} \tag{16}$$

$$\mathbf{T} = \mathbf{T}^T \tag{17}$$

where ρ is the density, **v** is the velocity field, t is time, **b** is the body force, and **T** is the stress tensor. It should be stated that the balance of angular momentum is in the absence of internal body forces.

MODEL DESCRIPTION

Whole Blood Constitutive Equation

As has already been discussed, blood is a shear-thinning viscoelastic fluid that stress-relaxes. The new constitutive equation can account for the shear-thinning viscosity, but fails to account for the stress-relaxation or elastic properties. Though flow is not taken into account in the biochemical portion of this work, the new equation for blood can be incorporated in future models. The stress for the new model is taken from Malek et al. (1995):

$$\boldsymbol{T} = -\pi \boldsymbol{I} + \mu_0 (1 + (2\mathbf{D})^2)^{\frac{p-2}{p}} (2\mathbf{D}) \quad (18)$$

where π is the pressure, $\boldsymbol{I}$ is the identity tensor, and $\mathbf{D}$ maintains its previous meaning. By setting p to a value less than two, shear-thinning fluids can be modeled. For this work, the equation was modified slightly to be:

$$\boldsymbol{T} = -\pi \boldsymbol{I} + \mu(c)(1 + \alpha(\mathbf{D})^{\mathbf{2}})^m (\mathbf{D}) \quad (19)$$

where $\mu(c)$ is a function based upon the amount of fibrin present in the blood, while α and m are constants. As levels of fibrin increase, the viscosity of blood also increases. When the level of fibrin within the blood reaches a critical level, for this work 350 nm, a clot is considered to be formed. The critical level is adapted from Ovanesov et al. (2002). At this concentration in the model, the viscosity will be 100 times that of normal blood.

The values for $\mu(0)$, α, and m are calculated based upon the experimental data

from Chien et al. (1966). The raw data points were extrapolated using Engauge Digitizer 4.1. By establishing axes and then clicking on individual plot points, the program accurately estimates values for raw data points. The function for $\mu(c)$ was then calculated assuming a parabolic relationship between the initial value and the critical value.

When solving for general viscosity in a rotary viscometer, the symmetric part of the velocity gradient is the shear rate. For whole blood, maintaining μ and α as already presented, eq 19 becomes:

$$\bar{\mu} = \mu(0)\left[1 + \frac{\alpha}{2}(\dot{\gamma})^2\right]^m \tag{20}$$

where $\bar{\mu}$ is the generalized viscosity and $\dot{\gamma}$ is the shear rate. Using MATLAB, the values for the constants were estimated and refined to match the raw data. The coefficient of determination was then used to calculate the accuracy of the fit. The coefficient of determination was found using:

$$R^2 = 1 - \frac{SS_{err}}{SS_{tot}} \tag{21}$$

where

$$SS_{err} = \sum (y_i - f_i)^2 \tag{22}$$

and

$$SS_{tot} = \sum (y_i - \hat{y})^2 \tag{23}$$

Here, y_i is the value obtained experimentally, $\hat{y}$ is the mean of all experimental values, and f_i is the predicted value using eq. 20.

Clotting Model

The aim of this work was to create a model that is more comprehensive in its approach while minimizing the increase in complexity. A full clotting model would include all three pathways of Virchow's Triad: the platelet pathway, the extrinsic pathway, and the intrinsic pathway. With respect to modeling, the platelet pathway involves many different elements interacting in various ways. Among these are: the activation of platelets by shear stress, activation of platelets by chemical agents, platelet transport in flowing blood, platelet-platelet and platelet-surface interaction mechanics and kinetics, and the interplay between the platelet pathway and the other pathways of coagulation. For these reasons, the platelet pathway was neglected in this work.

The in vitro case is considered where blood is exposed to a negatively charged surface as well as a layer of subendothelial proteins. This initiates both the intrinsic and extrinsic pathways of coagulation, which then proceed along the pathway of activation. The end result is a fibrin scaffold to which platelets would adhere over the thrombogenic layer. The formation of the clot then initiates a series of reactions that result in the breakdown of the clot.

The 28 equations for the production and depletion of the separate constituents are all of the form:

$$\frac{\partial [C_i]}{\partial t} + div([C_i]\mathbf{v}) = div\left(D_i \frac{\partial [C_i]}{\partial \mathbf{x}} \right) + G_i \tag{24}$$

Here, C_i is the concentration of each, D_i is the diffusion term correlating to that constituent, $\boldsymbol{v}$ is the velocity field of the fluid, $\mathbf{x}$ is the spatial dimension, and G_i is the

reaction term responsible for the production or depletion of the constituent in question. Because the velocity flow field is zero for this work, eq 21 reduces to:

$$\frac{\partial[C_i]}{\partial t} = div(D_i \frac{\partial[C_i]}{\partial \mathbf{x}}) + G_i \quad (25)$$

Figures 1 and 2 show a graphical representation of the reactions. The kinetic constants for the reactions can be found in Table 1, while the diffusion coefficients can be found in Table 2. The diffusion coefficients are calculated at 37˚ C using a correlation found in Young et al. (1980).

The 28 constituents chosen for this model are: fibrinogen (I) and fibrin (Ia), prothrombin (II) and thrombin (IIa), V and Va, VIII and VIIa, IX and IXa, X and Xa, tenase (IXa-VIIIa-PL^- written as Z), prothrombinase (Xa-Va-PL^- written as W), XI and XIa, XII and XIIa (also known as Hageman factor), prekallikrein and kallikrein (preK and Kalli), Antithrombin-III (ATIII), Protein C (PC) and Activated Protein C (APC), Tissue Factor Pathway Inhibitor (TFPI), C1-Inhibitor (C1INH), α_1-Antitrypsin (α_1AT), Tissue Plasminogen Activator (tPA), Plasminogen (PLS) and Plasmin (PLA) and α_2-Antiplasmin (α_2AP). Additionally, the TF-VIIa complex and endothelial cell tPA generation are taken into account in the boundary conditions. While not a complete list, these factors capture the salient features of the formation, propagation, and dissolution of a blood clot according to biochemical and clinical studies.

The equations for the reactions governing the production and depletion of each constituent are shown below. They are based upon experimental data from a multitude of sources. Zymogens are depleted by being activated into its corresponding active enzyme. The activated enzyme is then depleted by inactivation. Following convention, the terms

in brackets refer to a concentration of the factor located therein. The equations are:

$$G_{XIa} = \frac{k_{11}[IIa][XI]}{K_{11M}+[XI]} + \frac{k_{12a}[XIIa][XI]}{K_{12aM}+[XI]} - [XIa](h_{11A3}[ATIII] + h_{11L1}[\alpha_1 AT] + h_{CInh\text{-}11a}[C1INH]) \quad (26)$$

$$G_{XI} = \frac{-k_{11}[IIa][XI]}{K_{11M}+[XI]} + \frac{-k_{12a}[XIIa][XI]}{K_{12aM}+[XI]} \quad (27)$$

$$G_{XII} = \frac{-k_{12}[XII]}{K_{12M}+[XII]} + \frac{-k_{kalli}[kalli][XII]}{K_{kalliM}+[XII]} \quad (28)$$

$$G_{XIIa} = \frac{k_{12}[XII]}{K_{12}+[XII]} + \frac{k_{kalli}[Kalli][XII]}{K_{kalli}+[XII]} - [XIIa](h_{12} - h_{PCI\text{-}12a}[C1INH] - h_{ATIII}[ATIII] - h_{\alpha AP}[\alpha_2 AP]) \quad (29)$$

$$G_{preK} = \frac{-k_{PreKA}[XIIa][PreK]}{K_{PreKAM}+[PreK]} + \frac{-k_{PreKB}[XIIa][PreK]}{K_{PreKBM}+[PreK]} \quad (30)$$

$$G_{kalli} = \frac{k_{PreKA}[XIIa][PreK]}{K_{PreKAM}+[PreK]} + \frac{k_{PreKB}[XIIa][PreK]}{K_{PreKBM}+[PreK]} - h_{kalli}[Kalli] \quad (31)$$

$$G_{C1INH} = -[C1INH](h_{CInh\text{-}12a}[XIIa] + h_{CInh\text{-}11a}[XIa]) \quad (32)$$

$$G_{IXa} = \frac{k_9[XIa][IX]}{K_{9M}+[IX]} - h_9[IXa][ATIII] \quad (33)$$

$$G_{IX} = \frac{-k_9[XIa][IX]}{K_{9M}+[IX]} \quad (34)$$

$$[Z] = \frac{[VIIa][IXa]}{K_{dZ}} \quad (35)$$

$$G_{Xa} = \frac{k_{10}[VIIIa][Z]}{K_{10M}+[X]} - h_{10}[Xa][ATIII] - h_{TFPI}[TFPI][Xa] \quad (36)$$

$$G_X = \frac{-k_{10}[VIIIa][Z]}{K_{10M}+[X]} \tag{37}$$

$$[W] = \frac{[Va][Xa]}{K_{dW}} \tag{38}$$

$$G_{IIa} = \frac{k_2[W][II]}{K_{2M}+[II]} - h_2[IIa][ATIII] \tag{39}$$

$$G_{II} = \frac{-k_2[W][II]}{K_{2M}+[II]} \tag{40}$$

$$G_{VIIIa} = \frac{k_8[IIa][VIII]}{K_{8M}+[VIII]} - h_8[VIIIa] - \frac{h_{C8}[APC][VIIIa]}{H_{C8M}+[VIIIa]} \tag{41}$$

$$G_{VIII} = \frac{-k_8[IIa][VIII]}{K_{8M}+[VIII]} \tag{42}$$

$$G_{Va} = \frac{k_5[IIa][V]}{K_{5M}+[V]} - h_5[Va] - \frac{h_{C5}[APC][Va]}{H_{C5M}+[Va]} \tag{43}$$

$$G_V = \frac{-k_5[IIa][V]}{K_{5M}+[V]} \tag{44}$$

$$G_{APC} = \frac{k_{PC}[IIa][PC]}{K_{PCM}+[PC]} - h_{PC}[APC][\alpha_1 AT] \tag{45}$$

$$G_{PC} = \frac{-k_{PC}[IIa][PC]}{K_{PCM}+[PC]} \tag{46}$$

$$G_{ATIII} = -[ATIII](h_9[IXa] + h_{10}[Xa] + h_2[IIa] + h_{11A3}[XIa] + h_{ATIII}[XIIa]) \tag{47}$$

$$G_{TFPI} = -h_{TFPI}[TFPI][Xa] \tag{48}$$

$$G_{\alpha_1 AT} = -h_{PC}[APC][\alpha_1 AT] - h_{11L1}[XIa][\alpha_1 AT] \tag{49}$$

$$G_{Ia} = \frac{k_1[IIa][I]}{K_{1M} + [I]} - \frac{h_1[PLA][Ia]}{H_{1M} + [Ia]} \tag{50}$$

$$G_{I} = \frac{-k_1[IIa][I]}{K_{1M} + [I]} \tag{51}$$

$$G_{tPA} = 0 \tag{52}$$

$$G_{PLA} = \frac{k_{PLA}[tPA][PLS]}{K_{PLAM} + [PLS]} + \frac{k_{PLA-12a}[XIIa][PLS]}{K_{PLA-12aM} + [PLS]} - h_{PLA}[PLA][\alpha_2 AP] \tag{53}$$

$$G_{PLS} = \frac{-k_{PLA}[tPA][PLS]}{K_{PLAM} + [PLS]} - \frac{k_{PLA-12a}[XIIa][PLS]}{K_{PLA-12aM} + [PLS]} \tag{54}$$

$$G_{\alpha_2 AP} = -[\alpha_2 AP](h_{PLA}[PLA] + h_{\alpha AP}[XIIa]) \tag{55}$$

The equations thus far not included in previous models, and worthy of discussion, include 28, 29, 30, 31, and 32. These are the equations for the generation and depletion of factors XII, XIIa, prekallikrein, kallikrein, and C1-Inhibitor. Other equations have been adjusted as necessary to reflect the inclusion of these five species.

The activation of XIIa is triggered by contact with a negative surface. However, the work of Tankersley and Finlayson (1984) shows that, "...reciprocal activation is the predominant mode of factor XII activation in normal plasma." The auto-activation and activation by kallikrein both follow Michaelis-Menten kinetics. The initial activation uses high molecular weight kininogen (HMWK) as a cofactor. Here, it is assumed that there is plentiful HMWK for the reaction. When factor XII is activated, it splits into equal amounts of α-XIIa and β-XIIa. For this reason (and convenience), the single concentration of XIIa may be used with different kinetic constants to show its effect on

other species. Factor XIIa also contributes to the production of PLA following Michaelis-Menten kinetics, thus accelerating the process of fibrinolysis (Schousboe et al., 1999).

Factor XIIa is inactivated by ATIII, C1INH, and α_2AP following second order kinetics (Pixley et al. 1985). The inactivation constant for ATIII was obtained in the presence of saturating concentrations of heparin. The literature makes no distinction between the two forms of activated factor XII; therefore the inactivation is attributed to both.

Both forms of activated factor XII have an effect on kallikrein production with independent kinetic activation rates on prekallikrein. The production of kallikrein due to α-XIIa and β-XIIa follows Michaelis-Menten kinetics. This is reflected in equations 30 and 31. The inactivation follows pseudo-first order kinetics (Van der Graaf et al., 1983). Here, it is modeled as a first order reaction.

Protein C1-Inhibitor has been included because of its effect on the inactivation of factors XIIa, XIa, and Kallikrein. Though its concentration is not included in the deactivation of Kallikrein, the first order rate constant for Kallikrein decreases substantially in C1INH deficient plasma (Van der Graaf et al., 1983). Factors XIIa and XIa are both deactivated by C1INH following second order kinetics.

Boundary Conditions

The pressure and velocity of the fluid are maintained at zero throughout the simulation. The initial concentrations of all species are set as in Table 3. The activated enzymes start at 0.1% of their corresponding inactivated forms. With the exception of

the area for clot modeling, the concentrations at the wall are set at zero.

Within the area of clot development, the boundary conditions are set such that:

$$\frac{\partial[IXa]}{\partial x} = \frac{k_{7,9}[IX][TF-VIIa]}{K_{7,9M}+[IX]}\frac{L}{D_{IXa}} \tag{56}$$

$$\frac{\partial[IX]}{\partial x} = \frac{-k_{7,9}[IX][TF-VIIa]}{K_{7,9M}+[IX]}\frac{L}{D_{IX}} \tag{57}$$

$$\frac{\partial[Xa]}{\partial x} = \frac{-k_{7,10}[IX][TF-VIIa]}{K_{7,10M}+[X]}\frac{L}{D_{Xa}} \tag{58}$$

$$\frac{\partial[X]}{\partial x} = \frac{-k_{7,10}[IX][TF-VIIa]}{K_{7,10M}+[X]}\frac{L}{D_{X}} \tag{59}$$

$$\frac{\partial[tPA]}{\partial x} = -\left(k_{C-tPA}+k_{IIa-tPA}[IIa]+k_{Ia-tPa}[Ia]\right)[ENDO]\frac{L}{D_{tPA}} \tag{60}$$

For these equations, L is the length scale and chosen to be equal to the length (in the z-direction) of the clot; $D_{..}$ is the diffusion coefficient of the constituent of the subscript as listed in Table 2; the kinetic constants for the boundary conditions are listed in Table 4. The term *ENDO* represents endothelial cell concentration at the surface and is taken from Karsan and Harlan (2000):

$$[ENDO] = 2.0 \times 10^{9} \tag{61}$$

At the clotting surface, tissue factor associates with endogenous VIIa to form the TF-VIIa complex. As coagulation progresses, the action of thrombin also causes tissue factor and VIIa to associate and form TF-VIIa. In the work of Orfeo et al. (2005), 5 pM of tissue factor is introduced to synthetic plasma and the amount of TF-VIIa complex is

recorded. The curve is regenerated in Fig. 3, and scaled by a factor of 2×10^4 for the simulation. After 1500 seconds, the TF-VIIa level is set to zero.

For both simulations, gravity is not taken into account. Within the body, the directional effect of gravity changes due to several factors. As an example, if a person is standing, then gravity is working parallel to flow in arteries in the upper thigh. However, if a person sits or lies down, the gravity is working perpendicular to the direction of flow. Thus, if gravity were to be included it would call into question the physical position of a person. These models are neither developed nor intended for this level of specificity. It is also worth noting that the variation of position should not have a large impact on the formation and dissolution of a clot in a healthy subject. Therefore, gravity is not considered.

MATLAB Computational Methodology

Uniform clot formation, growth, and dissolution are considered in one spatial dimension in 2 mm deep quiescent plasma exposed to a negatively charged surface and a thrombogenic pane. Thus, both the intrinsic and extrinsic pathways of coagulation are activated. A clot is considered to be formed when fibrin concentration meets or exceeds 350 nM (adapted from Ovanesonov et al., 2002). The size of the clot is determined by tracking, in time, the regions within the domain that meet or exceed this level. The simulation is carried out over a period of 3000 seconds.

To model the information, the equations, initial conditions, and boundary conditions are non-dimensionalized according to:

$$t* = \frac{t}{T} \tag{62}$$

$$x* = \frac{x}{L} \tag{63}$$

$$C_i* = \frac{C_i}{C_i(t=0)} \tag{64}$$

$$D_i* = \frac{D_i T}{L^2} \tag{65}$$

$$G_i* = \frac{G_i T}{C_i(t=0)} \tag{66}$$

The non-dimensionalized equations are then solved using the 'pdepe' routine in MATLAB with a mesh of $\delta x^* = 0.005$, $\delta t^* = 0.001$, $T = 3000$, and $L = 0.002$.

Finite Domain Computational Methodology

Clot formation, growth, and dissolution are considered in a rigid cylindrical vessel 6 mm in diameter and 3 mm long. The pressure and velocity of the fluid are maintained at zero throughout the simulation. The calculations are done using the open source computational fluid dynamics program OpenFOAM. The software uses C++ and can be customized to reflect user-specific conditions. Additionally, the program comes with a mesh generation utility as well as post-processing tools to view results.

The solver was customized to reflect the biochemical equations described as well as the new constitutive equation for whole blood. The computations within the domain are carried out using a finite volume approach and a combination of two solution procedures. The first is the PISO (Pressure Implicit Splitting of Operators) algorithm, and it is used to solve time dependent equations. The second is the SIMPLE (Semi-Implicit Method for Pressure Linked Equations), and it is used for steady state equations.

The relevant files can be seen in Appendix D.

The mesh is created using the blockMesh utility that comes with the software. In it, vertices are created and then connected in three dimensions. The faces are then given properties (such as wall, inlet, outlet, and for this work, clot) and the internal mesh is created according to assigned specifications. Figures 4 and 5 show the mesh used in the calculation. Figure 6 shows the area subjected to the clotting boundary conditions.

The viscosity is calculated by using the fibrin concentration from the previous time step. As fibrin concentration increases past the critical level of clot development, the term is held constant. Thus, a clot is the maximum viscosity that the blood achieves.

The concentrations of the 28 biochemical factors have been set to a minimal level of 1×10^{-40} moles. Preliminary simulations showed values becoming negative numbers. As a result, this lower threshold was put in place to prevent such numerical discrepancies from happening.

RESULTS AND DISCUSSION

Constitutive Equation for Whole Blood

The constants for the equation have been obtained as well as the function $\mu(c)$. The initial point $\mu(0)$ is redefined for the initial condition of fibrin concentration such that $\mu(0) = \mu(7 \times 10^{-9})$. The equation for the function $\mu(c)$ is:

$$\mu(c) = 1.958^{15}[Ia]^2 + 0.1441 \quad (67)$$

The remaining constants are set as $\alpha = 1540$ and $m = -0.277$. Figure 7 shows the results of the model predictions (red) against experimental data (black) for whole blood. The behavior of the clot during formation ($\mu(150 \times 10^{-9})$) is compared to the clot ($\mu(350 \times 10^{-9})$) and whole blood ($\mu(7 \times 10^{-9})$) in Fig. 8.

The coefficient of determination for the whole blood model is $R^2 = 0.9938$. This shows that the whole blood model fits quite well to the experimental data. At low shear rates, the model is especially good at predicting the behavior of blood. Only at higher shear rates does a distinct and discernible difference become evident, and this is minimal. If flow were incorporated in the clotting model, these higher shear rates would fall outside the range for the size of the artery chosen (Kornet et al., 1999).

MATLAB Results

The non-dimensionalized equations have been calculated and the results for thrombin production, fibrin production, and clot size are presented in Fig. 9, 10, and 11, respectively. Thrombin production is monitored because it is the main activation agent of fibrin. A peak in thrombin values should not precede a maximum in fibrin

concentration, but rather serve as a harbinger of the apex. The results for the intrinsic and extrinsic pathway are compared to those of modeling just the extrinsic pathway taken from Anand et al. (2008). Figure 11 has already been presented in LaCroix and Anand (2010).

Including the intrinsic pathway causes thrombin production to reach a higher concentration, but a longer time period is needed to reach it. With the intrinsic pathway a maximum value of 1.967 nM is reached at a time of roughly 150 seconds. After initiation, the highest value the extrinsic pathway reaches is 1.35 nM at a time of about 75 seconds. Although, the extrinsic pathway peaks at an earlier time, it is worth noting that with the inclusion of the intrinsic pathway, a higher thrombin concentration is achieved at this same time. With the inclusion of the intrinsic pathway, maximum fibrin production achieves a higher value and occurs more quickly; a maximum concentration of 1723 nM is reached at roughly 300 seconds opposed to a peak of 1527 at roughly 400 seconds when only the extrinsic pathway is considered.

Figure 11 tracks the size of the clot throughout the domain considered. The inclusion of the intrinsic pathway shows not only a larger clot being formed, but a faster dissolution of the clot. This can be attributed to the increased rate of PLA production due to the inclusion of factor XIIa. The increase in PLA results in a quicker breakdown of fibrin, and thus a faster rate of fibrinolysis.

Finite Domain Results

The system of equations has been solved in a finite three dimensional domain with the boundary conditions stated. A clot is first developed at 440 seconds (the edges

of the clotting area reach a concentration level greater than 350 nM). At 475 seconds the entire clot boundary area has a concentration greater than 350 nM. Thus, a thrombus covers the entire clotting area. The thrombin level gradually increases until attaining a maximum value of 3.61 nM at a time of 528 seconds. After which, concentration drops off severely and stays at a low level for the remainder of the simulation. The peak level of thrombin within the clotting area with respect to time is shown in Fig. 12. The fibrin level within the clot area continues to increase until it reaches a maximum of 6123 nM at 1035 seconds. At this point, the clot begins to lyse until its level drops below 350 nM at 3685 seconds, signifying the dissolution of the clot at the wall. Figure 13 shows the maximum fibrin concentration within the clotting area for the duration of the simulation, and Fig. 14 shows the development of fibrin at 100 second intervals for the first 500 seconds. As can be seen, the area of fibrin concentration is higher at the edges and is reduced towards the center. Thus the clot is propagating inward from the outside edge. Figure 15 shows the radial view of the blood vessel at the time of maximum concentration of fibrin. This view shows how far the clot extends radially into the blood vessel.

In order to corroborate the simulation, the fibrin and thrombin levels were compared to experimental tests. It is difficult to obtain in-vivo clotting data, especially when considering the specificity of the problem as modeled. Two different experimental tests were used for model corroboration. For thrombin level, the work of Butenas et al. (1999) is used. In the experiment, the peak thrombin level is measured at 420 seconds; the peak level of thrombin in the simulation is achieved at 528 seconds. Similar to the

fibrin performance, this is slightly slow, but still acceptable. It is worth noting that the simulation within the finite domain matches the curve more closely than those of the MATLAB simulations.

For the fibrin, a study of temperature's effect on clotting done by Valeri et al. (1995) was used. The average clotting time for all subjects at a temperature of 37º C was 348 ± 78 seconds. The simulation performed shows the first signs of clot at 440 seconds, and the entire area being clotted at 475 seconds. The performance is lags slightly behind the experimental work, but remains comparable.

Sensitivity Analysis

A sensitivity analysis has been performed on prothrombin (factors Va and Xa). Prothrombin was chosen because it is the main activator of thrombin and would impact the production of fibrin through this relationship. For the original simulation, the activated factors are set to an initial level of 0.1% of their inactivated counterparts. The sensitivity analysis changed the initial level to 1%, and the impact on fibrin and thrombin production was recorded. The impact in relation to thrombin and fibrin production is presented in Fig. 16 and 17, respectively.

The sensitivity for the individual factors was also analyzed using:

$$S = \frac{\dfrac{\partial P}{P_{normal}}}{\dfrac{\partial M}{M_{0.1}}} \tag{68}$$

where the numerator is the difference in the maximum value of thrombin (or fibrin) achieved over the respective value in the original simulation. The denominator is the

change in the initial value of the individual factor over the initial value when it was at 0.1%. The equation normalizes the impact of the factors in question. The results are presented in Table 5. Increasing the initial concentration of either factor increases the maximum amount of fibrin produced. The impact on thrombin, however, is quite different. While increasing the initial concentration of factor Xa sees a significant increase in maximum thrombin produced, the adjustment to factor Va actually causes a reduction in this value. Using eq 68, factor Xa has the greatest positive impact on fibrin and thrombin production. However, this gives an incomplete picture.

The most obvious shortcoming of the sensitivity analysis above is the lack of temporal effects. Adjusting Va and Xa alone reduces the time of peak thrombin production from 528 to 428 and 486 seconds, respectively. When increased together, the time of peak thrombin production is 427 seconds. The time it took to achieve the minimum fibrin concentration for a clot as well as maximum fibrin and thrombin production is presented in Table 6. Increasing either Xa or Va not only increases the maximum fibrin concentration, but also reduces the time it takes to achieve this value. By setting the initial value of Va or Xa at 1%, the time to clot is reduced from 440 to 75 and 415 seconds, respectively. Increasing both values reduces this time further to 70 seconds. Thus, raising the initial level of Va to 1%, either by itself or in conjunction with Xa, has a great impact on the time it takes to develop a clot. This small increase reduces clotting time to $1/6^{th}$ of its initial value- a difference of more than 6 minutes.

Grid Dependence

A preliminary grid dependence test has been done, but a more thorough

study is necessary before any conclusive statements can be made. The aim of this work was to extend the current biochemical model to include the intrinsic pathway of activation rather than carry out a numerical study upon each of the factors involved and how they are affected by alterations to the size of the mesh. Such a study would be large in scope and encompass a great deal of numerics as well as error calculations.

For the grid dependence, the concentration of Va was monitored at a specific area, namely, the edge of the clot. Va was chosen because it is not one of the boundary values set and changes only due to reactions. A modest grid dependence test showed trivial changes in the concentration produced. A more drastic grid dependence test was completed by increasing the number of nodes for the mesh from 180 to 50,000. While the increase in nodes is by a factor of 270, the value of Va changes only by a factor of 3.3. These results show that a large jump in the number of nodes leads to a marginal increase in the concentration for factor Va. This modest addition is greatly offset by the huge expansion in computational time.

CONCLUSION AND FUTURE WORK

This dissertation has presented a variety of work to add to the established literature with regards to modeling blood and coagulation.

A new constituent equation for blood as it behaves in large arteries has been presented. The model is shear-thinning. The viscosity of the fluid is based upon fibrin concentration, a feature never before included in other models. Thus the viscosity is progressively increased dependent upon how much fibrin is present. Though flow was not utilized in the subsequent clotting simulation, this new blood model can (and will) be incorporated in all future simulations.

The intrinsic pathway has been added to already existing mathematical model of coagulation. This involved the inclusion of the relevant components as well as their respective rate constants for activation and deactivation. The result was the addition of five additional factors and the expansion of the number of partial differential equations from 23 to 28.

The newly expanded model for coagulation was then solved in one spatial dimension as well as in a finite three dimensional domain similar to a medium sized artery, such as the femoral artery. Both the formation and subsequent fibrinolysis of the clot were presented. This three dimensional model can be easily expanded to include flow characteristics of blood, and if so desired, more clotting factors.

Finally, sensitivity analysis was completed on select factors within the clotting cascade. Prothrombin, was examined by elevating initial concentrations of factors Va

and Xa separately as well as together. The results show that increasing the initial level of Va greatly reduces the time necessary for the formation of the clot, while a heightened level of Xa increases maximum fibrin and thrombin concentrations.

While the new constitutive equation marks a step towards a progressively more viscous fluid during coagulation, it fails to capture the other properties of blood, namely elasticity and stress relaxation. A more accurate model would model blood as a complex mixture of all of its constituents. Similarly, a clot would be modeled as a mixture of platelets adhering to the fibrin mesh and include the other many varied components found within the intravascular compartment.

The first step forward to a more accurate coagulation model is the inclusion of steady state flow. Though this is still not accurate with in-vivo conditions, it is the next step to a more complete model. Following the inclusion of steady state flow, the aspect of pulsatile flow can then be integrated. With this comes varying factors of pressure and velocity.

After the inclusion of flow, the third major pathway, the platelet pathway, can be integrated into the model. Because platelets can be activated by shear stress, it is logical to include flow prior to the inclusion of the platelet pathway. Its inclusion requires the mathematical characteristics of the interaction of both activated and inactivated platelets with each other as well as the other constituents being considered. Additionally, the model would consider the distribution qualities as well as platelet transport in flowing blood.

Finally, the finite dimensional model was calculated within a rigid cylinder.

Blood vessels expand and contract, and this may have a great effect on thrombus formation. Thus, the compliance of the blood vessel is an important aspect that would also need to be included for a fully complete simulation of blood coagulation.

In total, this dissertation marks a step, rather than a destination, on the long path towards a complete numerical simulation of blood coagulation.

REFERENCES

Ahmad, S., Rawalasheikh, R. Walsh, P.N., 1989. Comparative interactions of factor IX and factor-IXa with human platelets. J. Bio. Chem. 264 (6), 3244-3251.

Anand, M., Rajagopal, K., Rajagopal, K.R., 2003. A model incorporating some of the mechanical and biochemical factors underlying clot formation and dissolution in flowing blood. J. Theor. Med. 5 (3-4), 183-218.

Anand, M. Rajagopal, K.R., 2004. A shear thinning viscoelastic fluid model for describing the flow of blood. Int. J. Cardio. Med. Sci. 4 (2), 59-68.

Anand, M., Rajagopal, K., Rajagopal, K.R., 2008. A model for the formation, growth, and lysis of clots in quiescent plasma. A comparison between the effects of antithrombin III deficiency and protein C deficiency. J. Theor. Bio. 253, 725-738.

Baggiolini, M., Walz, A., and Kunkel, S.L.,1989. Neutrophil-activating peptide-1/interleukin 8, a novel cytokine that activates neutrophils**.** J. Clin. Invest. 84,1045–1049.

Bodnar, T., and Sequeira, A., 2008. Numerical simulation of the coagulation dynamics of blood. Comp. Math. Method. Med. 9 (2), 83-104.

Booth, N.A., 1995. Fibrinolysis and thrombosis. Bailliére Clin. Haem. 12 (3), 423-433.

Brummel-Ziedins, K., Orfeo, T. Jenny, N.S., Everse, S.J., Mann, K.G., 2004. Blood coagulation and fibrinolysis. In: Tkachuk, D.C., Hirschmann, J.V. (Eds.) Wintrobes Clinical Hematology, 11th ed. Lippincott, Williams, and Wilkins, Philadelphia, pp 677-690.

Bungay, S.D., Gentry, P.A., Gentry, R.D., 2003. A mathematical model of lipid-mediated thrombin generation. Math. Med. Biol. 20, 105-129.

Butenas, S., Veer, C., Mann, K.G., 1999. “Normal” thrombin generation. Blood 94(7), 2169-2178.

Chien, S. Usami, S., Taylor, H.M., Lundberg, J.L., Gregersen, M.I. 1966. Effects of hematocrit and plasma proteins on human blood rheology at low shear rates. J. Appl. Phys. 21(1), 81-87.

Chien, S., Usami, S., Dellenback, R.J., Gregersen, M.I., 1970. Shear dependent deformation of erythrocytes in rheology of human blood. Am. J. Phys. 219 (1) 136-142.

Cho, Y.I., Kensey, K.R., 1991. Effects of non-Newtonian viscosity of blood on flows in a diseased arterial vessel. Part 1: Steady flows. Biorheology 28(3-4), 241-262.

Colman, R.W., Clowes, A.W., George, J.N., Hirsh, J., Marder, V.J., 2001. Overview of hemostasis. In: Colman, R.W., Hirsh, J., Marder, V.J., Clowes, A.W., George, J.N. (Eds.), Hemostasis and Thrombosis, fourth ed. Lippincott, Williams and Wilkins, Philadelphia, pp. 1-16.

Davey, M.G., and Luscher, E.F., 1967. Actions of thrombin and other coagulant and proteolytic enzymes on blood platelets. Nature 216 (5118), 857-858.

Davie, E.W., and Ratnoff, O.D., 1964. Waterfall sequence for intrinsic blood clotting. Science 145, 1310-1312.

De Cristofaro, R., De Filippis, V., 2003. Interaction of the 268-282 region of glycoprotein ib alpha with the heparin-binding site of thrombin inhibits the enzyme activation of factor viii. Biochem. J. 373 (2), 593-601.

Diamond, S., Anand, S., 1993. Inner clot diffusion and permeation during fibrinolysis. Biophys. J. 65, 2622-2643.

Eckstein, E.C., and Belgacem, F., 1991. Model of platelet diffusion with drift and diffusion terms. Biophys. J. 60, 53-69.

Fåhraeus, R., and Lindqvist, T., 1931. The viscosity of the blood in narrow capillary tubes. Am. J. Physiol. 96, 562–568.

Freyssinet, J.M., Orfandoudakis, T.T., Ravant, C., Grunebaum, L., Gauchy, J., Cazenave, J.P., Wiesel, M.L., 1991. The catalytic role of anionic phospholipids in the activation of protein C by factor Xa and expression of its anticoagulant function in human plasma. Blood Coagul. Fibrin. 2, 691- 698.

Fung, Y.C., 1997. Biomechanics. Second ed. Springer-Verlag, New York.

Gailani, D., Broze, G.J., 1991. Factor XI activation in a revised model of blood coagulation. Science 253(5022), 909-912.

Gailani, D., Renné, T., 2007. Intrinsic pathway of coagulation on arterial thrombosis. Aerterioscler. Thromb. Vasc. Bio. 27, 2507-2513.

Goodnight, S. H., Hathaway, W.E., 2000. Disorders of Hemostasis and Thrombosis: A Clinical Guide. Second ed. McGraw-Hill, New York.

Heeb, M.J. Bischoff, R., Courtney, M., Griffin, J.H., 1990. Inhibition of activated protein C by recombinant α_1-antitrypsin variants with substitution of arginine or leucine for methionine. J. Biol. Chem. 265 (4), 2365-2389.

Johnston, B.M., Johnston, P.R., Corney, S., Kilpatrich, D., 2004. Non-Newtonian blood flow in human right coronary arteries: Steady state simulations. J. Biomech. 37 (5). 709-720.

Jones, K.C., Mann, K.G., 1994. A model for the tissue factor pathway to thrombin. II. A mathematical simulation. J. Biol. Chem. 269 (37), 23367-23373.

Kalafatis, M., Egan, J.O., vant Veer, C., Cawthern, K.M., Mann, K.G., 1997. The regulation of clotting factors. Crit. Rev. Eukar. Gene 7 (3), 241-280.

Karsan, A.L., Harlan, J.M., 2000. The blood vessel wall. In: Hoffman, R., Benz, E.J., Shattil, S.J., Furie, B., Cohen, H.J., Silberstein, L.E., McGlave, P. (Eds.), Hematology: Basic Principles and Practice, third ed. Churchill Livingstone, Philadelphia, 1770-1782.

Kesava, S., 2007. Red blood cells do more than just carry oxygen. New findings by NUS team show they aggressively attack bacteria too. *The Straits Times*. http://www.dbs.nus.edu.sg/eventlist/happenings/details/2007/dingSTsep07.pdf. retrieved 11 Nov 2007.

Khanin, M.A., Semenov, V.V., 1989. A mathematical model of the kinetics of blood coagulation. J. Theor. Biol. 136, 127-134.

Kolev, K., Lerant, I., Tenekkejiev, K., and Machovich, R., 1994. Regulation of fibrinolytic activity of neutrophil leukocyte elastase, plasmin, and miniplasmin by plasma protease inhibitors. J. Biol. Chem. 269 (25), 17030-17034.

Komiyama, Y., Pedersen, A.H., Kisiel, W., 1990. Proteolytic activation of human factors IX and X by recombinant human factor VIIa: effects of calcium, phospholipids, and tissue factor. Biochemistry-US 29 (40), 9418-9425.

Kornet, L., Hoeks, A.P.G., Lambregts, J., Reneman, R.S., 1999. In the femoral artery bifurcation, differences in mean wall stress within subjects are associated with different intima-media thickness. Arterio., Thromb., and Vasc. Biol. 19, 2933-2939.

Krishnaswamy, S., Church, W.R., Nesheim, M.E., Mann, K.G., 1987. Activation of human prothrombin by human prothrombinase. Influence of factor Va on the reaction mechanism. J. Biol. Chem. 262 (7), 3291-3299.

Kroll, M.H., Hellums, J.D., McIntire, L.V., Schafer, A.I., Moake, J.L., 1996. Platelets and Sheer Stress. Blood 88(5), 1525-1541.

Kuharsky, A., Fogelson, A.F., 2001. Surface mediated control of blood coagulation: The role of binding site densities and platelet deposition. Biophys. J. 80, 1050-1094.

LaCroix, D.E. and Anand, M., 2010. A model for the formation, growth, and dissolution of clots in vitro. Effect of the intrinsic pathway on antithrombin III deficiency and protein C deficiency, Recent Advances in Mechanics - Workshop in honor of Prof. K. R. Rajagopal on his 60th birthday, IIT Madras, Chennai, India.

Landmesser, U., Horning, B., and Drexler, H., (2004) Endothelial Function A Critical Determinant in Atherosclerosis?. Circulation 109, II-27-II-33.

Levin, E.G., Marzec, U., Anderson, J., Harker, L.A., 1984. Thrombin stimulates tissue plasminogen activator release from cultured human endothelial cells. J. Clin. Invest. 74, 1988-1995.

Luo, X.Y., Kuang, Z.B., 1992. A study on the constitutive equation of blood. J. Biomech. 25(8), 929- 934.

MacFarlane, R.G., 1964. An enzyme cascade in the blood clotting mechanism and its function as a biochemical amplifier. Nature 202, 498-499.

Madison, E.L., Coombs, G.S., Corey, D.R., 1995. Substrate-specificity of tissue-type plasminogen-activator- characterization of the fibrin-dependent specificity of t-PA for plasminogen. J. Biol. Chem. 270 (13), 7558-7562.

Malek, J., Rajagopal, K.R., Ruzicka, M., 1995. Existence and regularity of solutions and the stability of the rest state for fluids with shear dependent viscosity. Math. Mod. Meth. Appl. Sci. 5 (6), 789-812.

Mann, K.G., 1987. The assembly of blood clotting complexes on membranes. Trends Biochem. Sci. 12 (6), 229-233.

Mann, K.G., Gaffney, D., Bovill, E.G., 1995. Molecular biology, biochemistry, and lifespan of plasma coagulation factors. In: Beutter, B. (Ed.), fifth ed. Williams Hematology. McGraw-Hill, New York, pp. 1206-1226.

Martini, F.H., Ober, W.C., Garrison, C.W., Welch, K., Hutchings, R.T., 2001. Fundamentals of Anatomy and Physiology, Fifth ed. Prentice Hall, Upper Saddle River, pp. 692-750.

Meijers, J.C.M., Vlooswijk, R.A.A., Bouma, B.N., 1988. Inhibition of human blood coagulation factor XIa by C1 inhibitor. Biochemistry 27, 959-963.

Monkovic, D.D., Tracy, P.B., 1990. Functional characterization of human platelet-released factor V and its activation by factor Xa and thrombin. J. Biol. Chem. 265 (28), 17132-17140.

Nesheim, M.E., Tracy, R.P., Mann, K.G., 1984. "Clotspeed," a mathematical simulation of the functional properties of prothrombinase. J. Bio. Chem. 259 (3) 1447-1458.

Nemerson, Y., Gentry, R. 1986. An ordered addition, essential activation model of the tissue factor pathway of coagulation: evidence of a comformational cage. Biochemistry 25, 4020-4033.

Neuenschwander, P.F., Jesty, J., 1992. Thrombin-activated and factor Xa-activated human factor VIII: Differences in cofactor activity and decay rate. Arch. Biochem. Biophys. 296 (2), 426-434.

Obata, K., Mukai, K., Tsujimura, Y., Ishiwata, K., Kawan, Y., Minegishi, Y., Watanabe, N., and Karausuyama, H., 2007. Basophils are Essential Initiators of a Novel Type of Chronic Allergic Inflammation. Blood 110, 913-920.

Orfeo, T., Butenas, S., Brummel-Ziedins, K. E., Mann, K.G., 2005. The tissue factor requirement in blood coagulation. J of Bio. Chem. 280 (52), 42887-42896.

Ovanesov, M.V., Krasotkina, J.V., Ulyanova, L.I., Abushinova, K.V., Plyushch, O.P., Domogatskii, S.P., Vorobev, A.I., Ataullakhanov, F.I., 2002. Hemophilia a and b are associated with abnormal spatial dynamics of clot growth. BBA-Gen. Subjects 1572 (1), 45-57.

Pedley, T.J., 1980. The Fluid Mechanics of Large Blood Vessels. Cambridge University Press, Cambridge.

Pixley, R.A., Schapira, M., and Colman, R.W., 1985. The regulation of human factor XIIa by plasma proteinase inhibitors. J of Bio. Chem. 260 (3), 1723-1729.

Rajagopal, K., Lawson, J., 2007. Regulation of hemostatic system function by biochemical and mechanical factors. In: Mollica, F., Preziosi, L., Rajagopal, K.R. (Eds.), Modeling of Biological Materials. Birkhauser, Boston, pp. 179-210.

Rajagopal, K.R., Srinivasa, A.R., 2000. A thermodynamic framework for rate type fluid models. J. Non-Newt. Fluid Mech. 88, 207-227.

Rawalasheikh, R., Ahmed, S.S., Ashby, B., Walsh, P.N., 1990. Kinetics of coagulation factor X activation by platelet-bound factor IXa. Biochemistry-US 29 (10), 2606-2611.

Revak, S.D., Cochrane, C.G., Griffin, J.H., 1977. The binding and cleavage characteristics of human Hageman factor during contact activation: A comparison of normal plasma with plasmas deficient in factor XI, prekallikrein, or high molecular weight kininogen. J. Clin. Invest. 59, 1167-1175.

Rothenberg, M. E. and Hogan, S. P., 2006. The eosinophil. Annual Review of Immunology 24, 147-174.

Schousboe, I., Feddersen, K., Rojkjaer, R., 1999. Factor XIIa is a kinetically favorable plasminogen activator. Thromb. Haemost. 82, 1041-1046.

Schrauwen, Y., Kooistra, T., de Vries, R.E.M., Emies, J.J., 1995. Studies on the acute release of tissue-type plasminogen activator from human endothelial cells in vitro and in rats in vivo: Evidence for dynamic storage pool. Blood 85 (12), 3510-3517.

Scott, C.F., Schapira, M., James, H.L. Cohen, A.B., Colman, R.W., 1982. Inactivation of factor Xia by plasma protease inhibitors. J. Clin. Invest. 69 (12), 844-852.

Segal, Anthony W., 2005. How neutrophils kill microbes. Annual Review of Immunology 23, 197-223.

Silverberg, M. and Kaplan, A.P., 1982. Enzymatic activities of activated and zymogen forms of human hageman factor (factor XII). Blood 60 (1), 64-70.

Solymoss, S., Tucker, M.M., Tracy, P.B., 1988. Kinetics of inactivation of membrane-bound factor Va by activated protein C. J. Biol. Chem. 263 (29), 14884-14890.

Soons, H., Janssen-Claessen, T., Tans, G., Hemker, H.C., 1987. Inhibition of factor XIa by antithrombin III. Biochemistry-US 26 (15), 4624-4629.

Sun, Y., Gailani, D., 1996. Identification of factor IX binding site on the third apple domain of activated factor XI. J. Biol. Chem. 271 (46), 29023-29028.

Tankersly, D.L. and Finlayson, J.S., 1984. Kinetics of activation and autoactivation of human factor XII. Biochemistry 23, 273-279.

Thurston, G.B., 1972. Viscoelasticity of Human Blood. Biophys. J. 12 (9),1205-1217.

Tsiang, M., Paborsky, L.R., Li, W.X., Jain, A.K., Mao, C.T., Dunn, K.E., Lee, D.W., Matsumara, S.Y., Matteucci, M.D., Coutre, S.E., Leung, L.L.K., Gibbs, C.S., 1996. Protein engineering thrombin for optimal specificity and potency of anticoagulant activity in vivo. Biochemistry-US 34, 16449-16457.

Valeri, R.C., MacGregor, H., Cassidy, G., Tinney, R., Pompei, F., 1995. Effects of temperature on bleeding time and clotting time in normal male and female volunteers. Critical Care Medicine 23(4), 698-704.

Van der Graaf, F., Koedam, J.A., and Bouma, B.N., 1983. Inactivation of kallikrein in human plasma. J. Clin. Invest. 71 (1), 149-158.

Walburn, F.J., Schneck, D.J., 1976. A constitutive equation for whole human blood. Biorheology 13, 201-210.

Wald, G. Bownds, D., 1965. Reaction of rhodopsin chromophore with sodium borohydride. Nature 205 (4968). 254-257.

Wiebe, E.M., Stafford, A.R., Fredenburgh, J.C., Weitz, J.I., 2003. Mechanism of catalysis of inhibition of factor IXa by antithrombin in the presence of heparin or pentasaccharide. J. Biol. Chem. 278 (37), 35767-35774.

Yeleswarupu, K.K., 1996. Evaluation of continuum models for characterizing the constitutive behavior of blood. PhD Dissertation, University of Pittsburgh, Pittsburgh, PA, 1996.

Young, M.E., Carroad, P.A., Bell, R.L., 1980. Estimation of diffusion coefficients of proteins. Biotechnol. Bioeng. 22, 947-955.

Zarnitsina, V.I., Pokhilko, A.V. Ataullakhanov, F.I., 1996. A mathematical model for the spatio- temporal dynamics of intrinsic pathway of blood coagulation. I. The model description. Thromb. Res. 84 (4), 225-236.

APPENDIX A

FIGURES

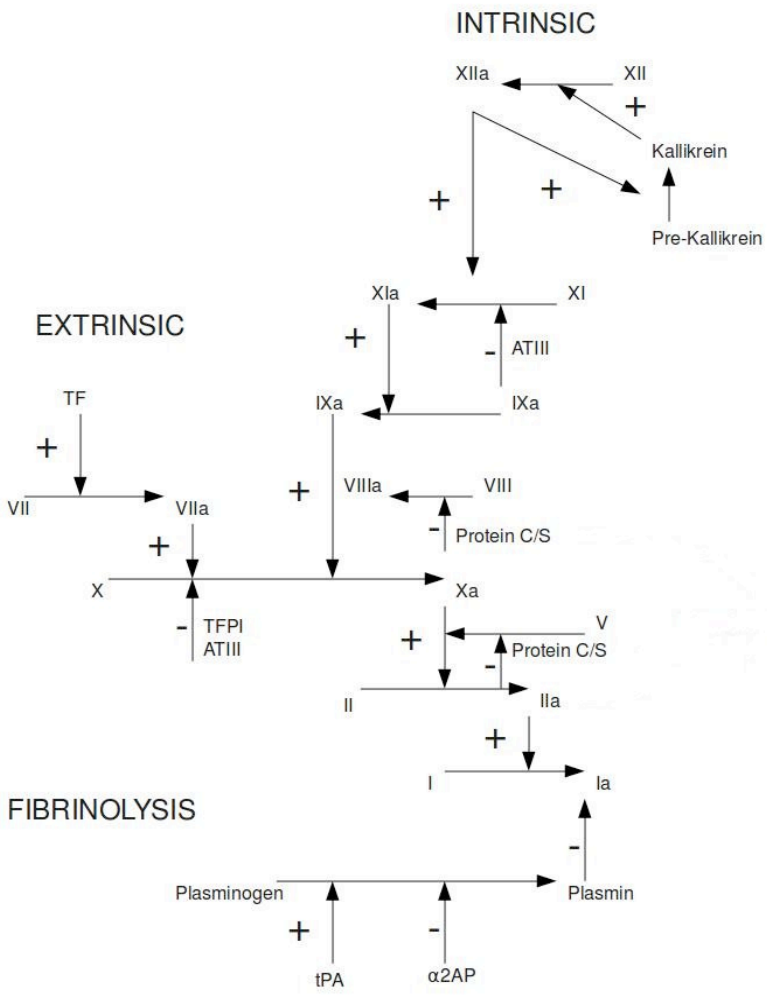

Fig. 1. Graphical representation of the clotting cascade that is modeled (the figure is modeled after a similar depiction from Rajagopal and Lawson, 2007).

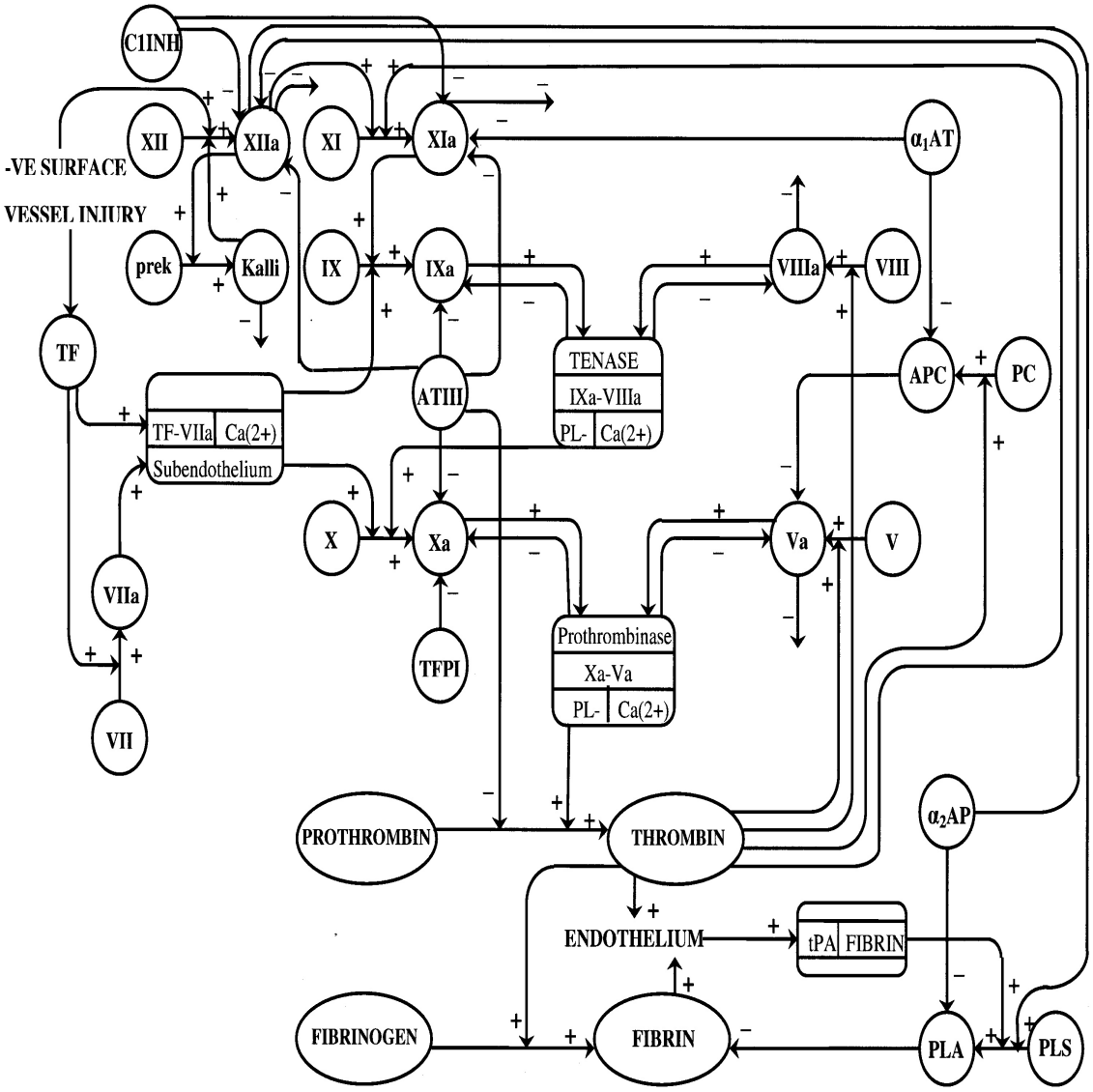

Fig. 2. Separate graphical depiction of the clotting cascade modeled. Included are the complexes formed by various factors and ions.(LaCroix and Anand, 2010).

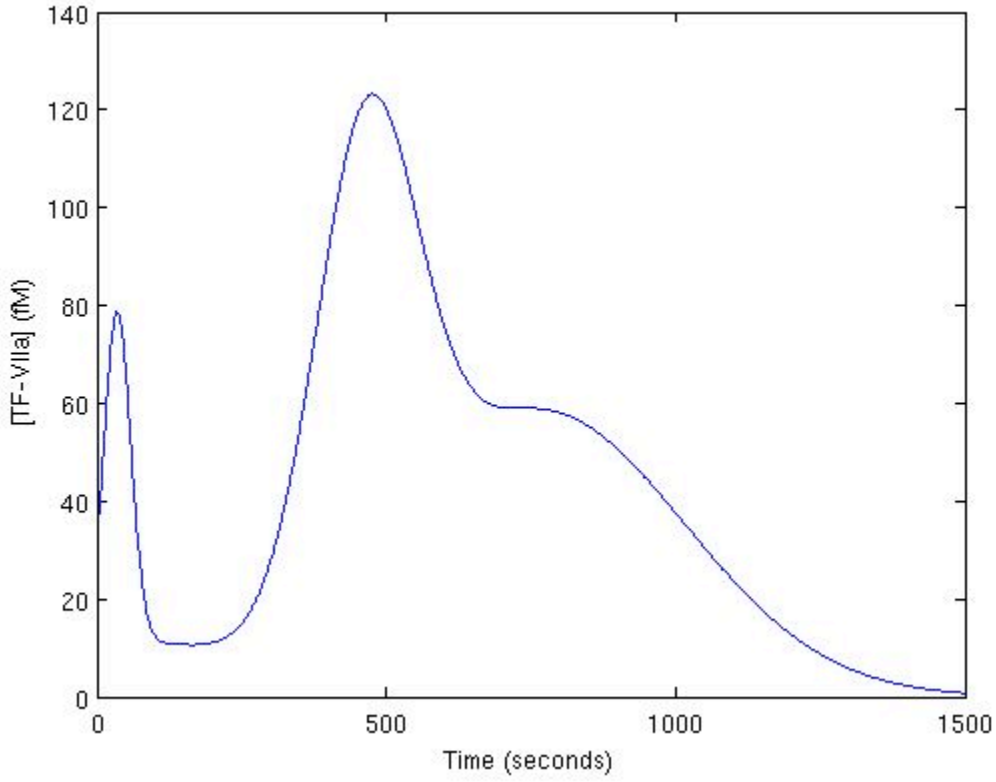

Fig. 3. Surface bound TF-VIIa concentration during thrombosis for 5 pM of added from tissue factor. The data is fitted to match the work of Orfeo et al. 2005.

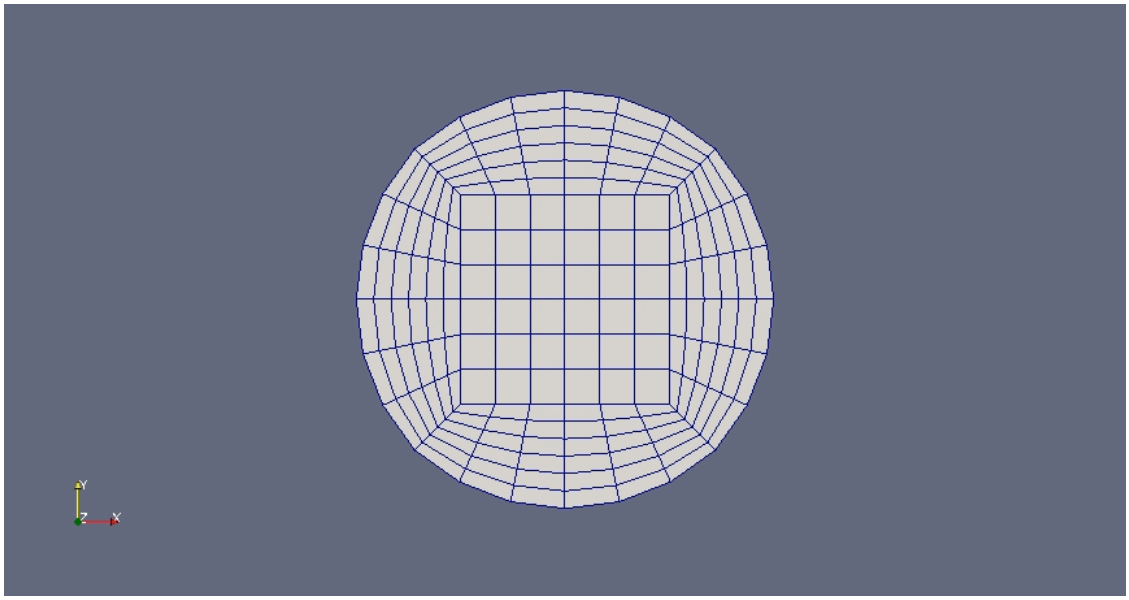

Fig. 4. Front view of the mesh used in calculation. The center of the mesh is a 6x6 square. Outside of this, each quadrant features a 6x6 section. There is a total of 18000 nodes.

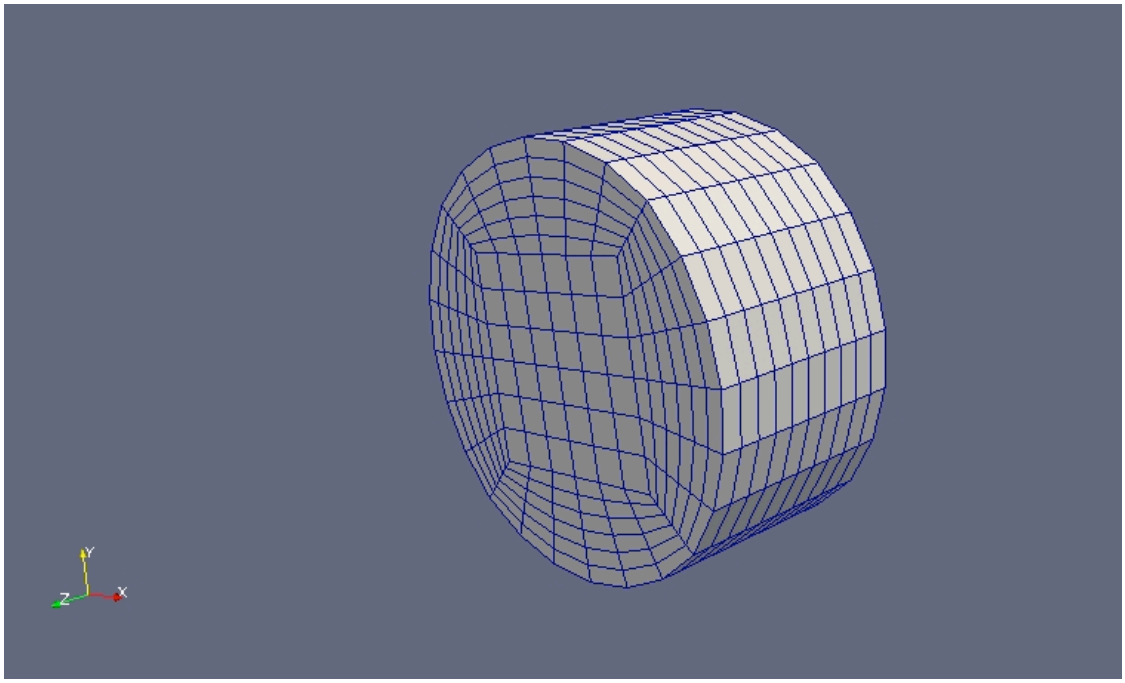

Fig. 5. A view of the mesh that includes all three dimensions.

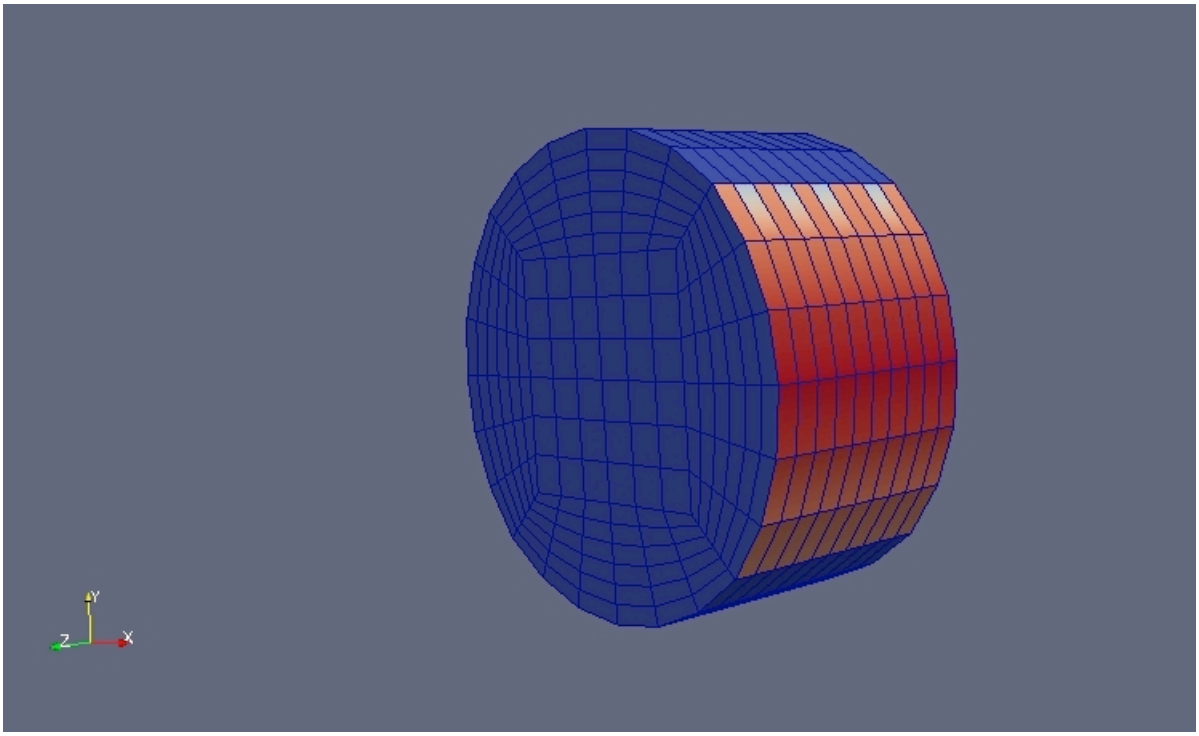

Fig. 6. The area subjected to the clotting boundary conditions is shown in red.

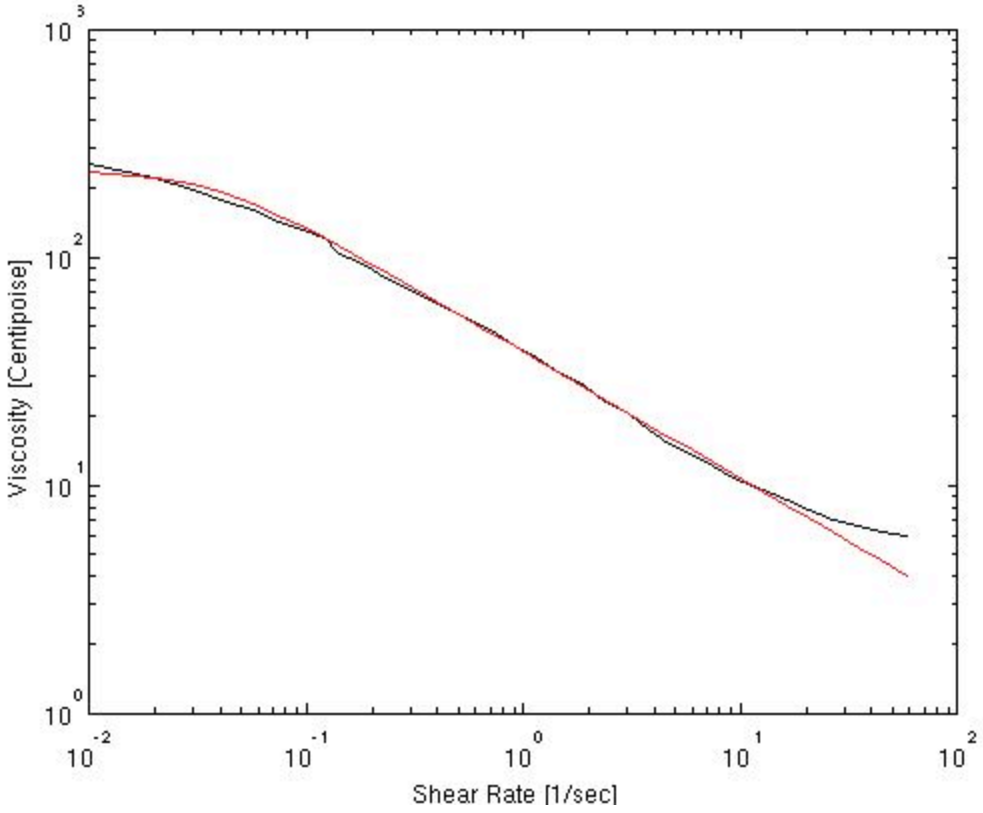

Fig. 7. Whole blood experimental data from Chien et al. 1966 (black) versus model predictions (red).

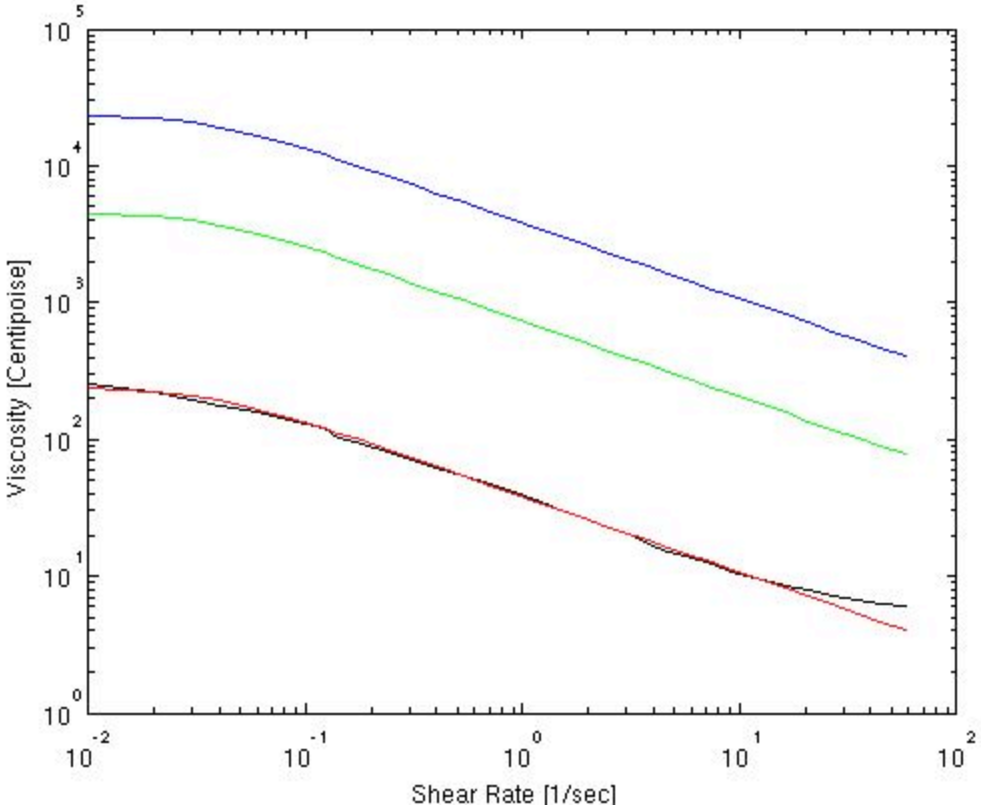

Fig. 8. Experimental data (black) from Chien et al. 1966 compared to $\mu(0)$ (red) to $\mu(150)$ (green) and $\mu(350)$(blue line). The blue line represents the behavior of a clot and is 100 times more viscous than whole blood.

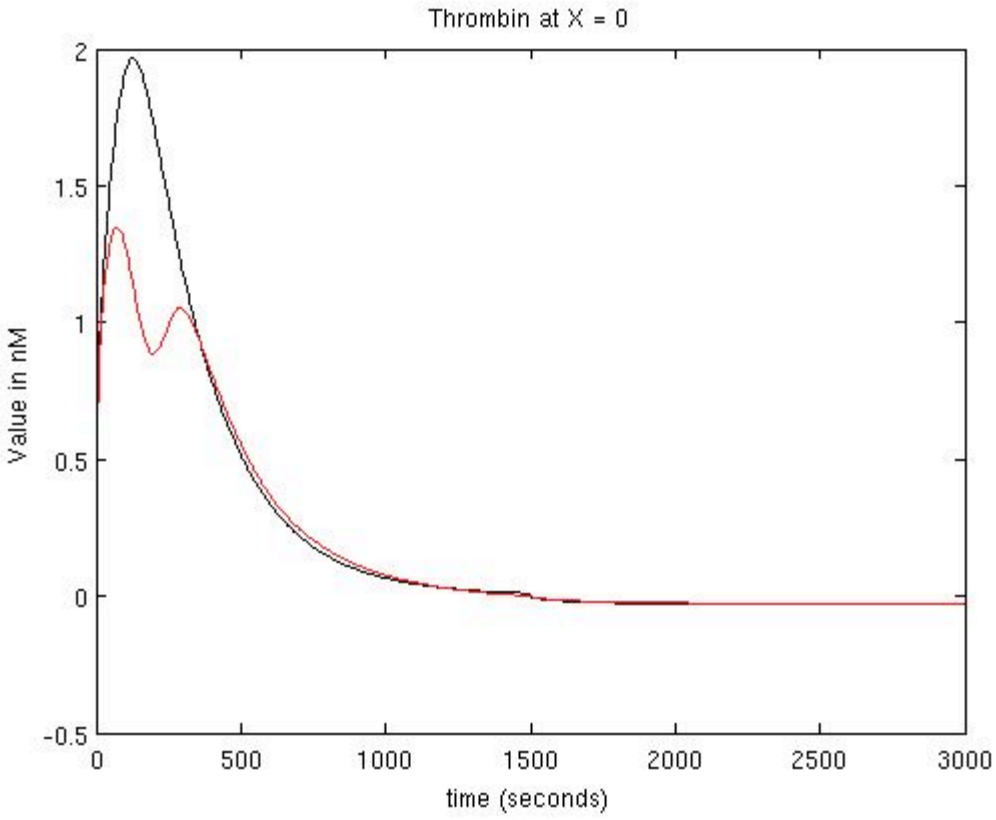

Fig. 9. Thrombin concentration at the clot surface versus time. The extrinsic model only is shown in red while the combined extrinsic and intrinsic pathways is modeled in black.

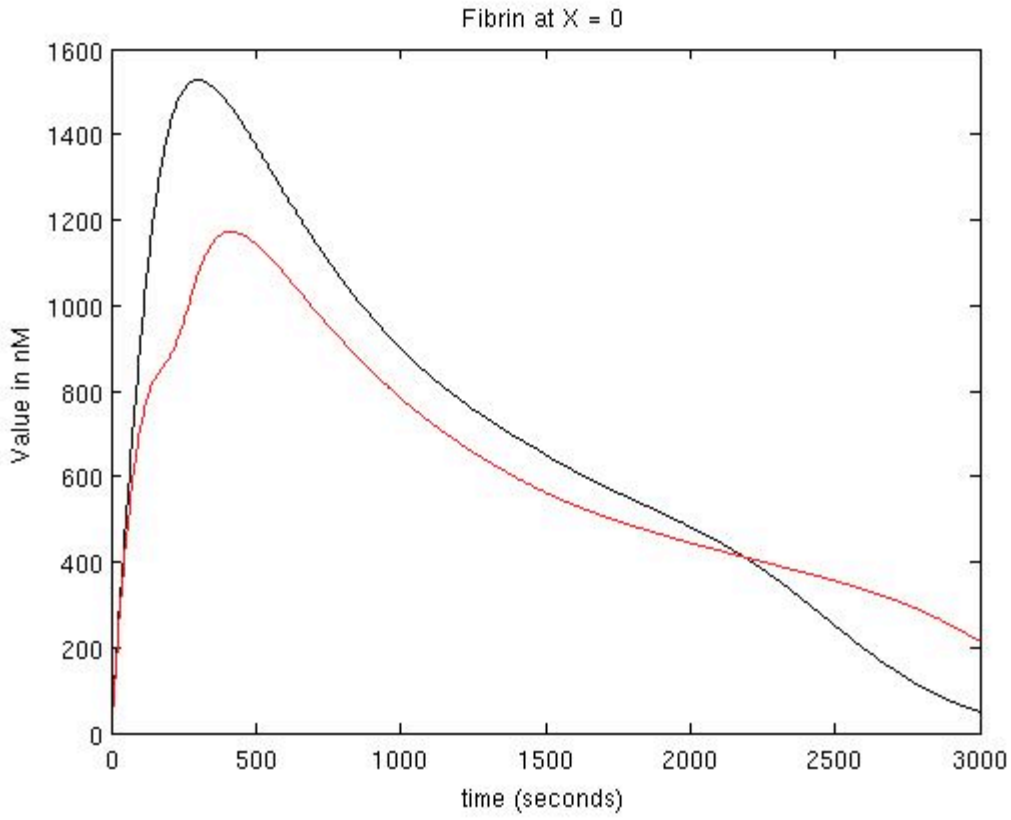

Fig. 10. Fibrin concentration at the clot surface versus time. The extrinsic pathway only is modeled in red while the combined extrinsic and intrinsic is modeled in black.

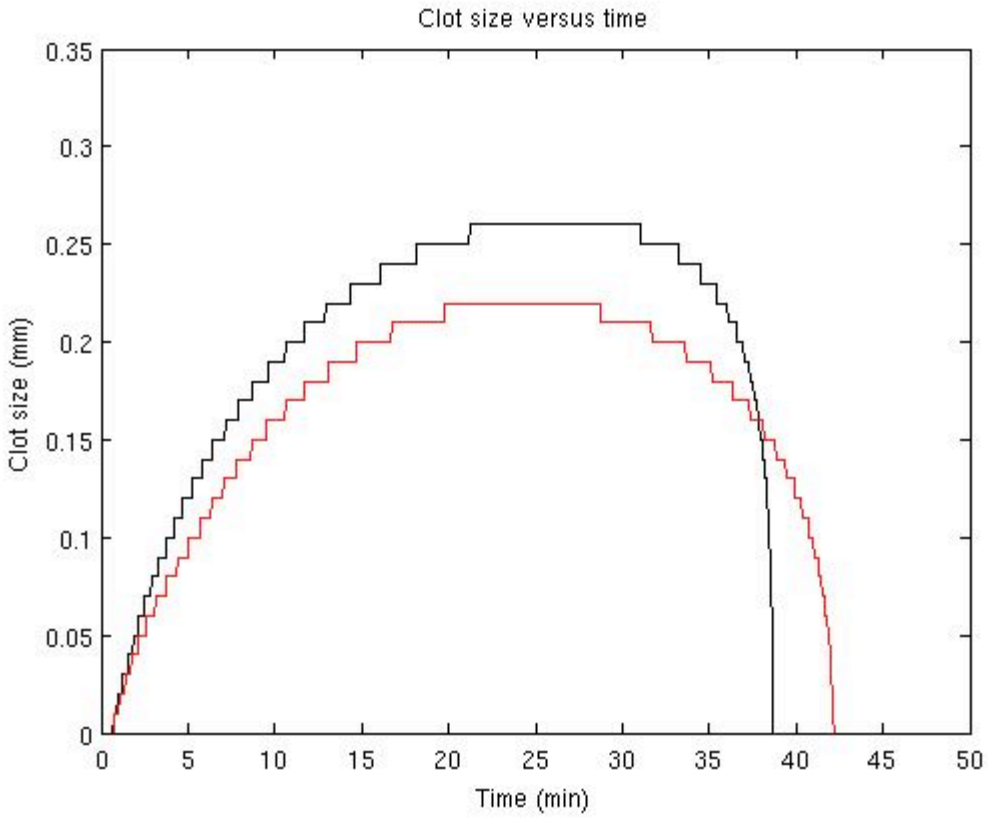

Fig. 11. Clot size versus time. The extrinsic pathway only is modeled in red. The extrinsic and intrinsic pathways combined are shown in black. (From LaCroix and Anand, 2010)

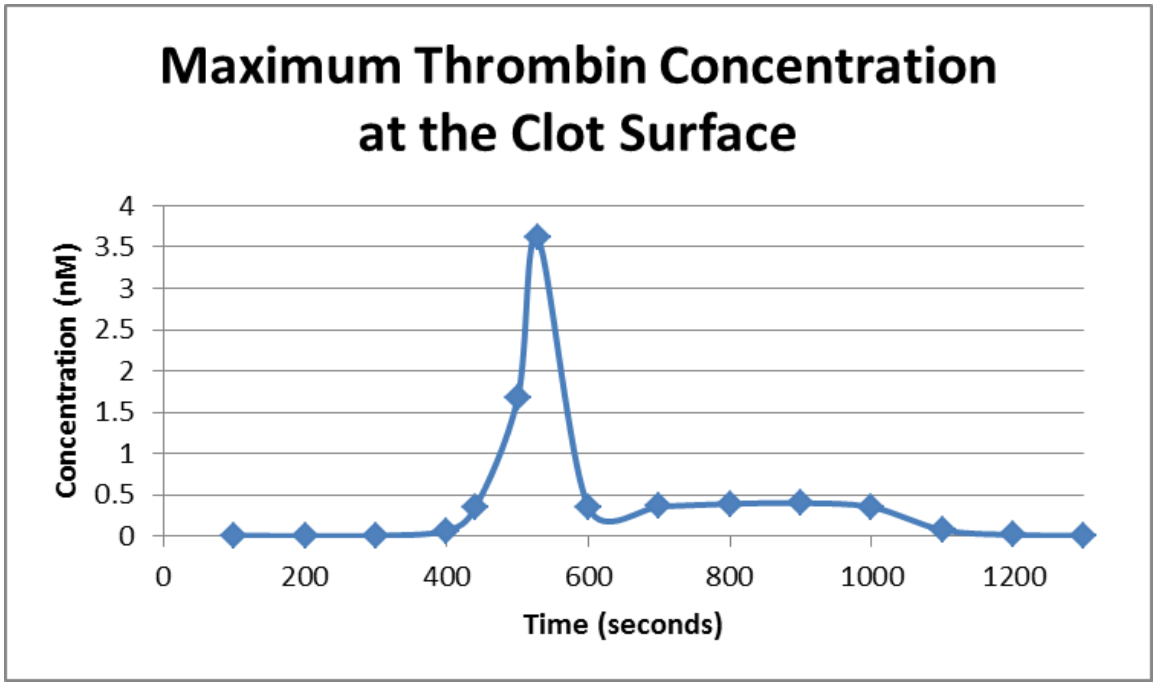

Fig. 12. The maximum value of thrombin on the clot surface for the first 1300 seconds. After 1300 seconds, the level drops to miniscule amounts. The maximum value of 3.61 nM is achieved at 528 seconds.

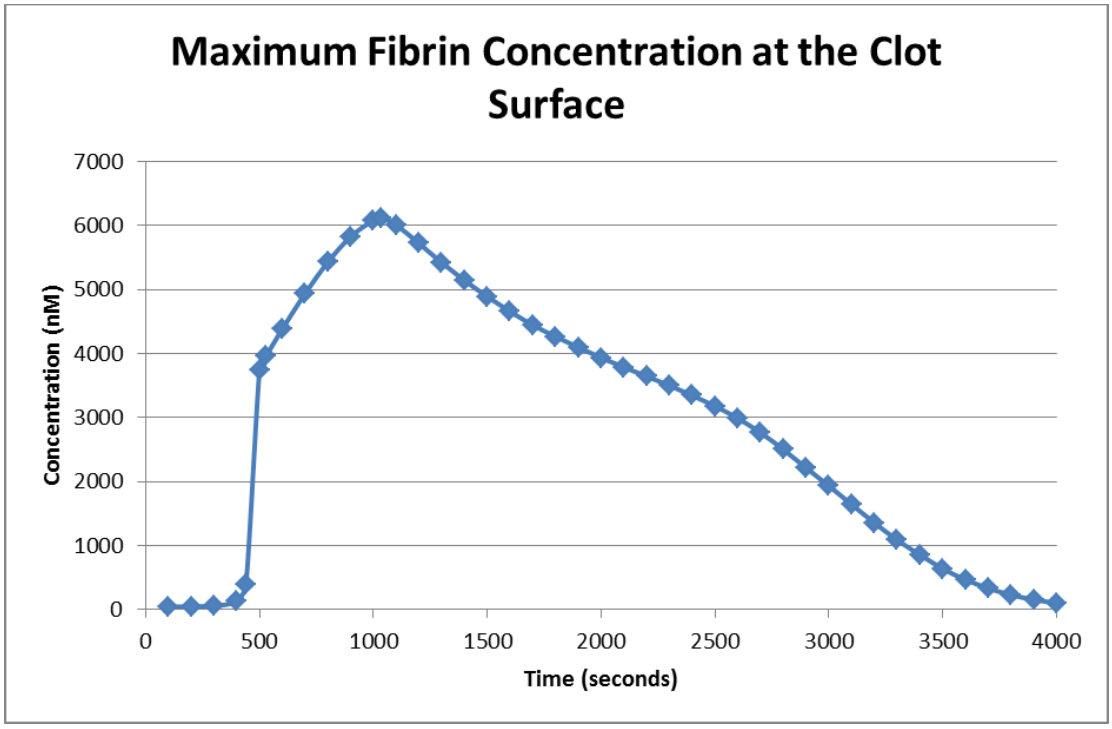

Fig. 13. Fibrin concentration at the clot surface throughout the simulation. A maximum value of 6123 nM is achieved at 1035 seconds, at which point lysis begins.

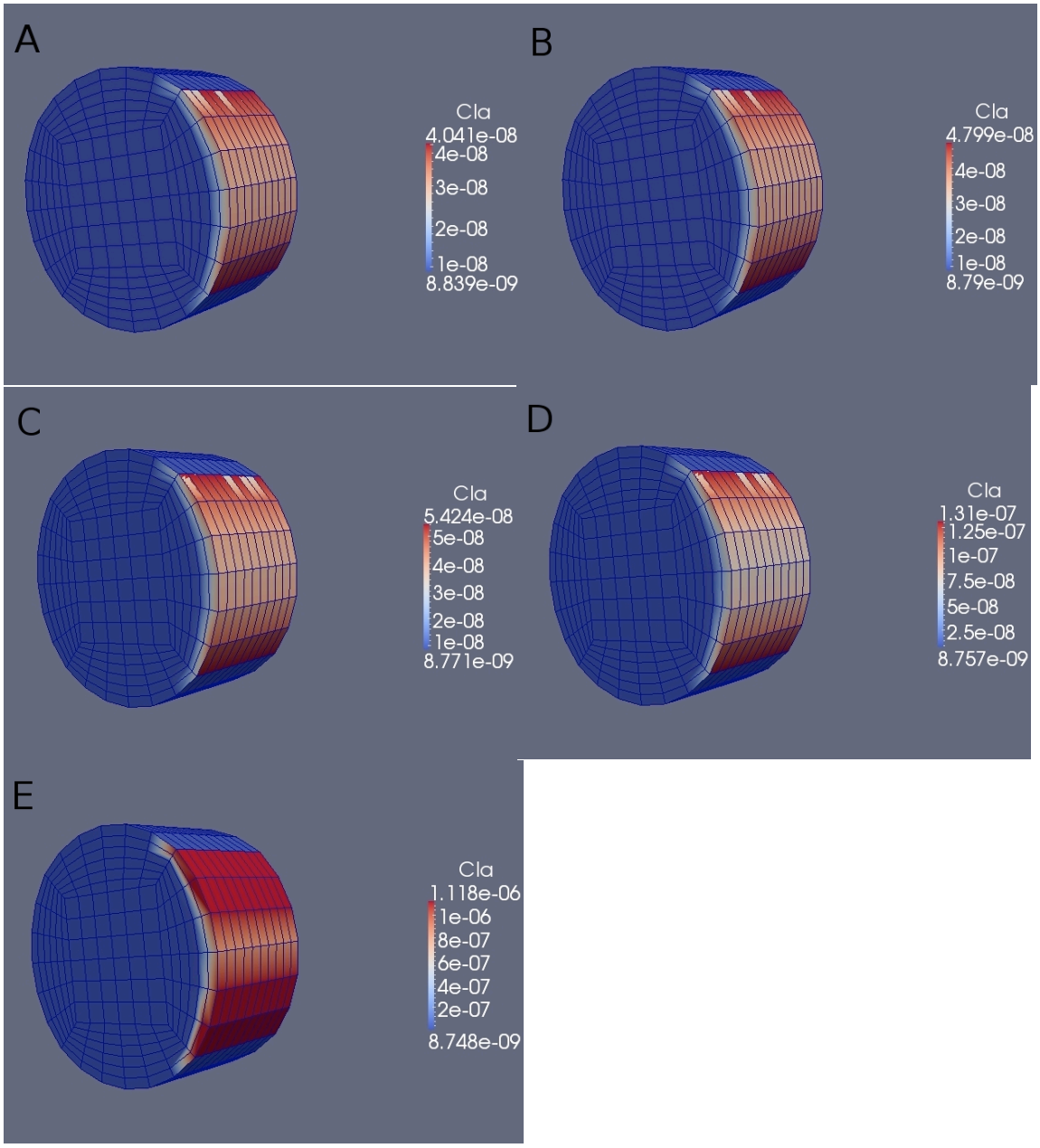

Fig. 14. Evolution of the clot for the first 500 seconds. The scales for concentration are different for each figure and are presented in moles (rather than nM). The time at each (in seconds) is 100 (A), 200 (B), 300 (C), 400 (D), and 500 (E). Notice that between (D) and (E), the a concentration above 350 nM is achieved everywhere over the clotting surface.

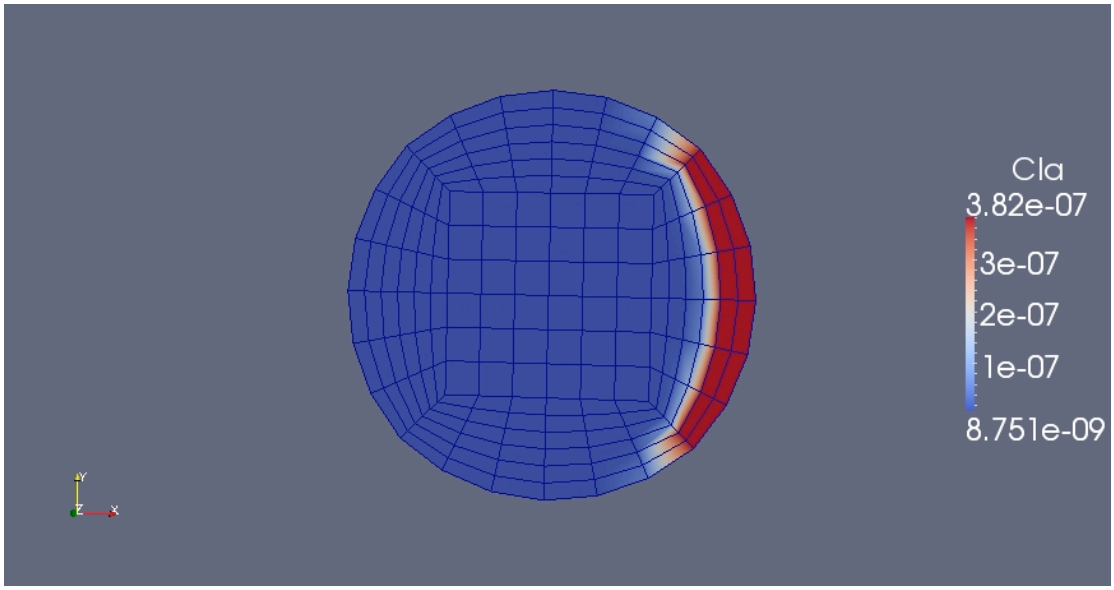

Fig. 15. The radial size of the clot at peak fibrin concentration.

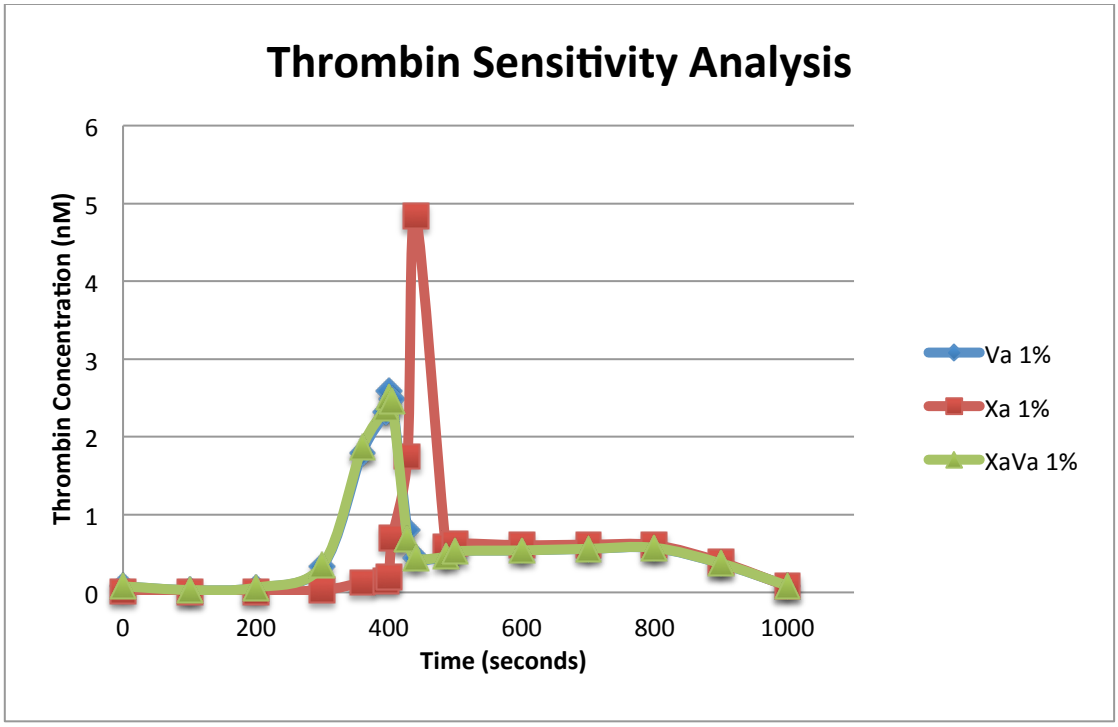

Fig. 16. Maximum thrombin concentration on the clot surface for different initial conditions. "Va 1%," and "Xa 1%," refer to the initial level of each being raised to 1%; and "XaVa 1%" represents both concentrations being at an elevated level. Increasing factor Va lowers the maximum amount of thrombin produced, however it reduces the time it takes to reach this maximum. By only increasing the initial level of Xa, a higher maximum is produced quicker, though not as quick as increasing Va.

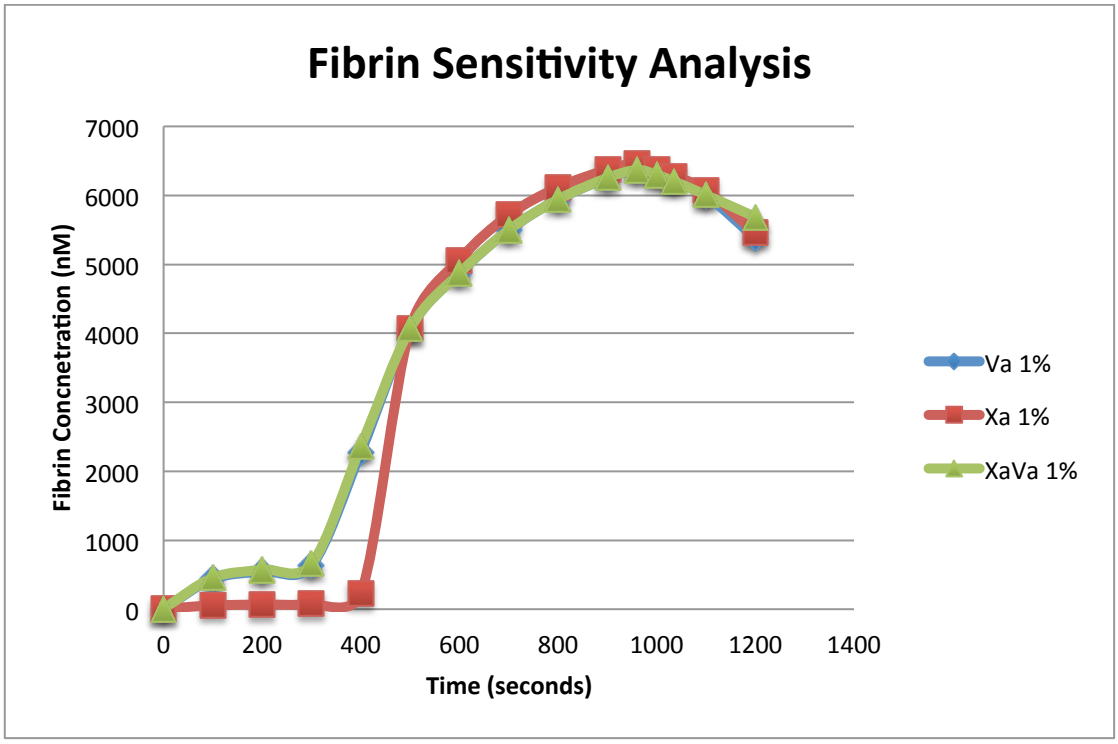

Fig. 17. Maximum fibrin concentration at the surface of the clot for different initial conditions. "Va 1%," and "Xa 1%," refer to the initial level of each being raised to 1%; and "XaVa 1%" represents both concentrations being at a heightened level. The "Va 1%" and "XaVa 1%" line follow the same path. While each increases the maximum fibrin produced, the biggest difference is in the initiation stage where an increased level of factor Va (either by itself or in conjunction with Xa) leads to a much quicker formulation of a clot.

APPENDIX B

TABLES

Table 1
Kinetic constants used for the biochemical equations. "M" is for Michaelis-Menten, "F" is for first order and "S" is for second order.

Equation	Kinetics	Parameters	Source
26, 27	M	k_{11} = 0.0078 min^{-1}, K_{11M} = 50 nM	Gailani and Broze (1991)
26,47	S	h_{11A3} = 1.6 x 10^{-3} nM^{-1} min^{-1}	Soons et al. (1987)
26, 49	S	h_{11L1} = 11.3 x 10^{-5} nM^{-1} min^{-1}	Scott et al. (1982)
33, 34	M	k_{9} = 11 min^{-1}, K_{9M} = 160 nM	Sun and Gailani (1996)
33, 47	S	h_{9} = 0.0162 nM^{-1} min^{-1}	Wiebe et al. (2003)
41,42	M	k_{8} = 194.4 min^{-1}, K_{8M} = 112 000 nM	De Cristofaro and De Filippis (2003)
41	F	h_{8} = 0.222 min^{-1}	Neuenschwander and Jesty (1992)
41	M	h_{C8} = 10.2 min^{-1} , H_{C8M} = 12.6 nM	Anand et al. (2008)
35	S	K_{dZ} = 0.56 nM	Ahmad et al. (1989)
43, 44	M	k_{5} = 27.0 min^{-1}, K_{5M} = 140.5 nM	Monkovic and Tracy (1990)
43	F	h_{5} = 0.17 min^{-1}	Freyssinet et al. (1991)
43	M	h_{C5} = 10.2 min^{-1}, H_{C5M} = 14.6 nM	Solymoss et al. (1988)
36, 37	M	k_{10} = 2391 min^{-1} , K_{10M} = 160 nM	Rawalasheikh et al. (1990)
36, 47	S	h_{10} = 0.347 nM^{-1} min^{-1}	Wiebe et al. (2003)
36, 48	S	h_{TFPI} = 0.48 nM^{-1} min^{-1}	Wiebe et al. (2003)
38	S	K_{dW} = 0.1 nM	Mann (1987)
39, 40	M	k_{2} = 1344 min^{-1} , K_{2M} = 1060 nM	Krishnaswamy et al. (1987)
39, 47	S	h_{2} = 0.714 nM^{-1} min^{-1}	Wiebe et al. (2003)
45,46	M	k_{PC} = 39 min^{-1} , K_{PCM} = 1060 nM	Tsiang et al. (1996)
45,49	S	h_{PC} = 6.6 x 10^{-7} nM^{-1} min^{-1}	Heeb et al. (1990)
50,51	M	k_{1} = 3540 min^{-1} , K_{1M} = 3160 nM	Tsiang et al. (1996)
50	M	h_{1} = 1500 min^{-1} , H_{1M} = 250 000 nM	Diamond and Anand (1993)
53, 54	M	k_{PLA} = 12 min^{-1}, K_{PLAM} = 18 nM	Madison et al. (1995)
53, 55	S	h_{PLA} = 0.096 nM^{-1} min^{-1}	Kolev et al. (1994)
28, 29	M	k_{12} = 19.8 min^{-1}, K_{12M} = 7500 nM	Tankersly and Finlayson (1984)
28, 29	M	k_{kalli} = 435 min^{-1}, K_{kalliM} = 780 nM	Tankersly and Finlayson (1984)
30, 31	M	k_{PreKA} = 216 min^{-1}, K_{PreKAM} = 91 nM	Tankersly and Finlayson (1984)
30, 31	M	k_{PreKB} = 2400 min^{-1}, K_{PreKBM} = 36,000 nM	Tankersly and Finlayson (1984)
29	F	h_{12} = 0.85 min^{-1}	Silverberg and Kaplan (1982)
29, 32	S	$h_{Clnh\text{-}12a}$ = 2.2 x 10^{-4} nM^{-1} min	Pixley et al. (1985)
29, 55	S	$h_{\alpha AP}$ = 1.1 x 10^{-5} nM^{-1} min^{-1}	Pixley et al. (1985)

Table 2
Diffusion coefficients.

Species	Mol. Mass (Da)	(cc/g)	Diffusion coefficient (cm^2/sec)
I	340000	0.723	3.10×10^{-7}
Ia	≈660,000	0.730	2.47×10^{-7}
II	72000	0.719	5.21×10^{-7}
IIA	37000	0.730	6.47×10^{-7}
V	330000	0.730	3.12×10^{-7}
Va	179000	0.730	3.82×10^{-7}
VIII	330000	0.730	3.12×10^{-7}
VIIIa	166000	0.730	3.92×10^{-7}
IX	56000	0.730	5.63×10^{-7}
Ixa	41000	0.730	6.25×10^{-7}
X	56000	0.730	5.63×10^{-7}
Xa	25000	0.730	7.37×10^{-7}
XI	16000	0.730	3.97×10^{-7}
XIa	80000	0.730	5.0×10^{-7}
XII	80000	0.730	5.0×10^{-7}
XIIa	108000	0.730	2.93×10^{-7}
preK	84000	0.730	4.92×10^{-7}
Kalli	84000	0.730	4.92×10^{-7}
C1INH	105000	0.730	4.61×10^{-7}
PC	62000	0.730	5.44×10^{-7}
APC	60000	0.730	5.50×10^{-7}
ATIII	58000	0.730	5.57×10^{-7}
TFPI	40000	0.730	6.30×10^{-7}
α_1AT	51000	0.728	5.82×10^{-7}
tPA	68000	0.730	5.28×10^{-7}
PLS	92000	0.715	4.81×10^{-7}
PLA	85000	0.715	4.93×10^{-7}
α_2AP	70000	0.720	5.25×10^{-7}

Table 3
Initial conditions for all factors.

Species	Initial Concentration (nM)	Source
I	7000	Mann et al. (1995)
Ia	7.0	
II	1400	Mann et al. (1995)
IIa	1.4	
V	20	Mann et al. (1995)
Va	0.02	
VIII	0.7	Mann et al. (1995)
VIIIa	0.0007	
IX	90	Mann et al. (1995)
IXa	0.09	
X	170	Mann et al. (1995)
Xa	0.17	
XI	30	Bungay et al. (2003)
XIa	0.03	
XII	500	Brummel-Ziedens et al. (2004)
XIIa	5	
preK	485	Brummel-Ziedens et al. (2004)
Kalli	4.85	
C1INH	1625	Brummel-Ziedens et al. (2004)
PC	60	Mann et al. (1995)
APC	.06	
ATIII	3400	Kalafatis et al. (1997)
TFPI	2.5	Mann et al. (1995)
α_1AT	45000	Colman et al. (2001)
tPA	0.08	Booth (1995)
PLS	2180	Lijnen and Collen (2000)
PLA	2.18	
α_2AP	105	Colman et al. (2001)

Table 4
Boundary condition parameters.

Species	Parameter
	$k_{7,9} = 32.4\ min^{-1}$, $K_{7,9M} = 24\ nM$
	$k_{7,10} = 103.0\ min^{-1}$, $K_{7,10M} = 240\ nM$
tPA (Constitutive)	$k_{C\text{-}tPA} = 6.52\ nM\ m^2\ min^{-1}$
tPA (Thrombin-induced)	$k_{IIa\text{-}tPA} = 9.27 \times 10^{-12}\ e^{-134.8(t-t0)} m^2\ min^{-1}$
tPA (Fibrin-induced)	$k_{Ia\text{-}tPA} = 5.059 \times 10^{-18} m^2\ min^{-1}$

Table 5
Sensitivity, S, to increased initial levels of activated factors V and X. The initial condition is set to 1% of their respective inactivated forms. The table uses equation 58 from the text to find the impact of raising Va and Xa individually and together.

Factor	**Ia**	**IIa**
Va	0.004	-0.034
Xa	0.006	0.039
XaVa	0.0045	-0.025

Table 6
Temporal effects of adjusting the initial level of Va and Xa. The time it takes to achieve the maximum concentration of fibrin and thrombin as well as reach a fibrin concentration of 350 nM (time to clot) is listed. For thrombin and fibrin, the maximum values are included in parentheses. All times listed are in seconds.

Factor	Ia	IIa	Time to Clot
Va	960 (6364)	428 (2.49)	75
Xa	960 (6464)	486 (4.84)	415
XaVa	960 (6369)	427 (2.46)	75
Normal	1025 (6123)	528 (3.61)	440

APPENDIX C

Model	Apparent Viscosity

Walburn and Schneck(1976)

$$\mu = C_1 e^{HC_2}[e^{C_4\left(\frac{TPMA}{H^2}\right)}](\dot{\gamma})^{-C_3 H}$$

C_1=.00797 C_2 = 0.0608
C_3 = .00499 C_4 = 14.585
H = 40% TPMA = 25.9

Carreau (Cho and Kensey, 1991) $\mu = \mu_\infty + (\mu_0 - \mu_\infty)[1 + (\lambda\dot{\gamma})^2)]^{\frac{n-1}{2}}$

λ= 3.313 n = 0.3568
μ_0 = 0.56P μ_∞ = 0.0345P
P represents pressure

Casson (Fung, 1997) $\mu = [(\eta^2 J_2)^{\frac{1}{4}} + 2^{\frac{-1}{2}}\tau_y^{\frac{1}{2}}]^2 \; J_2^{\frac{-1}{2}}$

$|\dot{\gamma}| = \frac{2}{J_2} \quad \tau_y = 0.1(0.625H)^3$

$\eta = \eta_0(1 - H)^{-2.5}$
η_0 = 0.012P H = 0.037

P represents pressure

Luo and Kang (1992) $\mu = \frac{\tau}{\dot{\gamma}} = \eta_1 + \eta_2\dot{\gamma}^{-\frac{1}{2}} + \tau_y\dot{\gamma}^{-1}$

τ_y = 4.968 η_1 = 4.076
η_2 = 16.066

Refined Oldroyd-B (Anand and Rajagopal, 2004)

$$\mu = \frac{\frac{\mu_1 \lambda}{\chi} + \eta_1}{2}$$

$$\lambda = \frac{1}{[1+\frac{1}{4\chi^2}(\dot{\gamma})^2]^{1/3}}$$

$$\chi = K[\frac{2\dot{\gamma}^2}{4\chi^2} \frac{1}{1+\frac{\dot{\gamma}^2}{4\chi^2}}]^n$$

n = 0.1372 η_1 = 0.1 Pa s^{-1}

μ_1 = 0.1611 N/m^2 K = 58.0725 s^{-1}

APPENDIX D

Files are separated by bold font introducing them. There are four files presented.

chemPimpleFoam.C :

```
/*---------------------------------------------------------------------------*\
  =========                 |
  \\      /  F ield         | OpenFOAM: The Open Source CFD Toolbox
   \\    /   O peration     |
    \\  /    A nd           | Copyright held by original author
     \\/     M anipulation  |
-------------------------------------------------------------------------------
License
    This file is part of OpenFOAM.

    OpenFOAM is free software; you can redistribute it and/or modify it
    under the terms of the GNU General Public License as published by the
    Free Software Foundation; either version 2 of the License, or (at your
    option) any later version.

    OpenFOAM is distributed in the hope that it will be useful, but WITHOUT
    ANY WARRANTY; without even the implied warranty of MERCHANTABILITY or
    FITNESS FOR A PARTICULAR PURPOSE.  See the GNU General Public License
    for more details.

    You should have received a copy of the GNU General Public License
    along with OpenFOAM; if not, write to the Free Software Foundation,
    Inc., 51 Franklin St, Fifth Floor, Boston, MA 02110-1301 USA

Application
    pimpleFoam

Description
    Large time-step transient solver for incompressible, flow using the PIMPLE
    (merged PISO-SIMPLE) algorithm.

    Turbulence modelling is generic, i.e. laminar, RAS or LES may be selected.

\*---------------------------------------------------------------------------*/

#include "fvCFD.H"
#include "singlePhaseTransportModel.H"
#include "turbulenceModel.H"
```

```
// * * * * * * * * * * * * * * * * * * * * * * * * * * * * * * * * * * * * * * * * * //

int main(int argc, char *argv[])
{
    #include "setRootCase.H"
    #include "createTime.H"
    #include "createMesh.H"
    #include "createFields.H"
    #include "initContinuityErrs.H"

    Info<< "\nStarting time loop\n" << endl;

    while (runTime.run())
    {
        #include "readTimeControls.H"
        #include "readPIMPLEControls.H"
        #include "CourantNo.H"
        #include "setDeltaT.H"

        runTime++;

        Info<< "Time = " << runTime.timeName() << nl << endl;

        // --- Pressure-velocity PIMPLE corrector loop
        for (int oCorr=0; oCorr<nOuterCorr; oCorr++)
        {
            if (nOuterCorr != 1)
            {
                p.storePrevIter();
            }

//          Info<< "Velocity:" << endl;
            #include "UEqn.H"
//          Info<< "Chemical:" << endl;
                #include<chemEqs.H>
//          Info<< "Viscoelasticity:" << endl;
//              #include<viscoElasticity.H>


            // --- PISO loop
            for (int corr=0; corr<nCorr; corr++)
            {
                #include "pEqn.H"
```

```
            }

            turbulence->correct();
        }

//      if(runTime.write()){nuF.write();}
        runTime.write();

        Info<< "ExecutionTime = " << runTime.elapsedCpuTime() << " s"
            << "  ClockTime = " << runTime.elapsedClockTime() << " s"
            << nl << endl;
    }

    Info<< "End\n" << endl;

    return 0;
}


//
*********************************************************************
** //
```

Where, UEqn.H :

```
nuST = ((nu0 - nuInf)/pow(scalar(1) + pow(lambdaMCM*mag(symm(fvc::grad(U))),
m),n) + nuInf)/rho;

nuF = min(nuST*(1 + nuStar*mag(CIa)/Threshold_CIa),
nuST*nuStar*mag(CIa)/mag(CIa));


tmp<fvVectorMatrix> UEqn
(
    fvm::ddt(U)
  + fvm::div(phi, U)
  - fvm::laplacian(nuF, U)
//  - fvc::div(Te)/rho

//  + turbulence->divDevReff(U)
);

if (oCorr == nOuterCorr-1)
```

```
{
   UEqn().relax(1);
}
else
{
   UEqn().relax();
}

volScalarField rUA = 1.0/UEqn().A();

if (momentumPredictor)
{
   if (oCorr == nOuterCorr-1)
   {
      solve(UEqn() == -fvc::grad(p), mesh.solver("UFinal"));
   }
   else
   {
      solve(UEqn() == -fvc::grad(p));
   }
}
else
{
   U = rUA*(UEqn().H() - fvc::grad(p));
   U.correctBoundaryConditions();
}
************************************************************************
************
```

PEqn.H :

```
U = rUA*UEqn().H();

if (nCorr <= 1)
{
   UEqn.clear();
}

phi = (fvc::interpolate(U) & mesh.Sf())
   + fvc::ddtPhiCorr(rUA, U, phi);

adjustPhi(phi, U, p);
```

```
// Non-orthogonal pressure corrector loop
for (int nonOrth=0; nonOrth<=nNonOrthCorr; nonOrth++)
{
    // Pressure corrector
    fvScalarMatrix pEqn
    (
        fvm::laplacian(rUA, p) == fvc::div(phi)
    );

    pEqn.setReference(pRefCell, pRefValue);

    if
    (
        oCorr == nOuterCorr-1
     && corr == nCorr-1
     && nonOrth == nNonOrthCorr
    )
    {
        pEqn.solve(mesh.solver("pFinal"));
    }
    else
    {
        pEqn.solve();
    }

    if (nonOrth == nNonOrthCorr)
    {
        phi -= pEqn.flux();
    }
}

#include "continuityErrs.H"

// Explicitly relax pressure for momentum corrector except for last corrector
if (oCorr != nOuterCorr-1)
{
    p.relax();
}

U -= rUA*fvc::grad(p);
U.correctBoundaryConditions();

************************************************************************
```

****

And chemEqs.H is :

/*There will be set of following advection-diffusion equations:

DC/Dt = D*ddC/dxx + G

28 constituents:

CI
CIa
CII
CIIa
CV
CVa
CVIII
CVIIIa
CIX
CIXa
CX
CXa
CXI
CXIa
CPC
CAPC
CATIII
CTFPI
Calpha1AT
CtPA
CPLS
CPLA
Calpha2AP
CXII
CXIIa
CCInh
CCInh
CKalli */

```
//1
   tmp<fvScalarMatrix> CIEqn
   (
           fvm::ddt(CI)
         + fvm::div(phi, CI)
         - fvm::laplacian(DCI, CI)
            + fvm::Sp((k1)*CIIa/(K1M + CI),CI)


            //         - (-k1)*CIIa*CI/(K1M + CI)
   );


   CIEqn().relax();
   solve(CIEqn);
   CI = max(CI,  1e-40);
   Info<< "CI min:" << min(CI).value() << endl;
   Info<< "CI max:" << max(CI).value() << endl;
//2
   tmp<fvScalarMatrix> CIaEqn
   (
           fvm::ddt(CIa)
         + fvm::div(phi, CIa)
         - fvm::laplacian(DCIa, CIa)
            - (k1*CIIa*CI/(K1M + CI))
            + fvm::Sp(h1*CPLA/(H1M + CIa),CIa)

            //- (k1*CIIa*CI/(K1M + CI) - h1*CPLA*CIa/(H1M + CIa)   )
   );
   CIaEqn().relax();
   solve(CIaEqn);
   CIa = max(CIa,  1e-40);
   Info<< "CIa min:" << min(CIa).value() << endl;
   Info<< "CIa max:" << max(CIa).value() << endl;
//3
   tmp<fvScalarMatrix> CIIEqn
   (
           fvm::ddt(CII)
         + fvm::div(phi, CII)
         - fvm::laplacian(DCII, CII)
            + fvm::Sp((k2)*CVa*CXa/(KdW*(K2M + CII)),CII)
```

```
            // - (-k2)*CVa*CXa*CII/(KdW*(K2M + CII))
    );
    CIIEqn().relax();
    solve(CIIEqn);
    CII = max(CII,  1e-40);
    Info<< "CII min:" << min(CII).value() << endl;
    Info<< "CII max:" << max(CII).value() << endl;
//4
    tmp<fvScalarMatrix> CIIaEqn
    (
            fvm::ddt(CIIa)
          + fvm::div(phi, CIIa)
          - fvm::laplacian(DCIIa, CIIa)
             - k2*CVa*CXa*CII/(KdW*(K2M + CII))
             + fvm::Sp(h2*CATIII,CIIa)

            //   - (k2*CVa*CXa*CII/(KdW*(K2M + CII)) - h2*CIIa*CATIII)
    );
    CIIaEqn().relax();
    solve(CIIaEqn);
    CIIa = max(CIIa,  1e-40);
    Info<< "CIIa min:" << min(CIIa).value() << endl;
    Info<< "CIIa max:" << max(CIIa).value() << endl;
//5
    tmp<fvScalarMatrix> CVEqn
    (
            fvm::ddt(CV)
          + fvm::div(phi, CV)
          - fvm::laplacian(DCV, CV)
             + fvm::Sp((k5*CIIa/(K5M + CV)),CV)

             //- (-k5*CIIa*CV/(K5M + CV))
    );
    CVEqn().relax();
    solve(CVEqn);
    CV = max(CV,  1e-40);
    Info<< "CV min:" << min(CV).value() << endl;
    Info<< "CV max:" << max(CV).value() << endl;
//6
    tmp<fvScalarMatrix> CVaEqn
    (
            fvm::ddt(CVa)
          + fvm::div(phi, CVa)
          - fvm::laplacian(DCVa, CVa)
```

```
            - (k5*CIIa*CV/(K5M + CV))
            + fvm::Sp(h5,CVa)
            + fvm::Sp(hC5*CAPC/(HC5M + CVa),CVa)

            //- (k5*CIIa*CV/(K5M + CV) - h5*CVa - hC5*CAPC*CVa/(HC5M + CVa) )
    );
    CVaEqn().relax();
    solve(CVaEqn);
    CVa = max(CVa,  1e-40);
    Info<< "CVa min:" << min(CVa).value() << endl;
    Info<< "CVa max:" << max(CVa).value() << endl;
//7
    tmp<fvScalarMatrix> CVIIIEqn
    (
          fvm::ddt(CVIII)
        + fvm::div(phi, CVIII)
        - fvm::laplacian(DCVIII, CVIII)
            + fvm::Sp((k8*CIIa/(K8M + CVIII)),CVIII)

            //- (-k8*CIIa*CVIII/(K8M + CVIII))
    );
    CVIIIEqn().relax();
    solve(CVIIIEqn);
    CVIII = max(CVIII,  1e-40);
    Info<< "CVIII min:" << min(CVIII).value() << endl;
    Info<< "CVIII max:" << max(CVIII).value() << endl;
//8
    tmp<fvScalarMatrix> CVIIIaEqn
    (
          fvm::ddt(CVIIIa)
        + fvm::div(phi, CVIIIa)
        - fvm::laplacian(DCVIIIa, CVIIIa)
            - ((k8*CIIa*CVIII/(K8M + CVIII)))
            + fvm::Sp(h8,CVIIIa)
            + fvm::Sp(hC8*CAPC/(HC8M + CVIIIa) ,CVIIIa)

            //- (k8*CIIa*CVIII/(K8M + CVIII) - h8*CVIIIa - hC8*CAPC*CVIIIa/(HC8M
+ CVIIIa) )
    );
    CVIIIaEqn().relax();
    solve(CVIIIaEqn);
    CVIIIa = max(CVIIIa,  1e-40);
    Info<< "CVIIIa min:" << min(CVIIIa).value() << endl;
    Info<< "CVIIIa max:" << max(CVIIIa).value() << endl;
```

```
//9
   tmp<fvScalarMatrix> CIXEqn
   (
            fvm::ddt(CIX)
          + fvm::div(phi, CIX)
          - fvm::laplacian(DCIX, CIX)
             + fvm::Sp((k9*CXIa/(K9M + CIX)),CIX)

             //- (-k9*CXIa*CIX/(K9M + CIX))
   );

   CIXEqn().relax();
   solve(CIXEqn);
   CIX = max(CIX,  1e-40);
Info<< "CIX min:" << min(CIX).value() << endl;
Info<< "CIX max:" << max(CIX).value() << endl;

//10
   tmp<fvScalarMatrix> CIXaEqn
   (
            fvm::ddt(CIXa)
          + fvm::div(phi, CIXa)
          - fvm::laplacian(DCIXa, CIXa)
             - (k9*CXIa*CIX/(K9M + CIX))
             + fvm::Sp(h9*CATIII,CIXa)

             //- (k9*CXIa*CIX/(K9M + CIX) - h9*CIXa*CATIII)
   );
   CIXaEqn().relax();
   solve(CIXaEqn);
   CIXa = max(CIXa,  1e-40);
   Info<< "CIXa min:" << min(CIXa).value() << endl;
   Info<< "CIXa max:" << max(CIXa).value() << endl;
//11
   tmp<fvScalarMatrix> CXEqn
   (
            fvm::ddt(CX)
          + fvm::div(phi, CX)
          - fvm::laplacian(DCX, CX)
             + fvm::Sp((k10*CVIIIa*CIXa/(KdZ*(K10M + CX))),CX)


             //- (-k10*CVIIIa*CIXa*CX/(KdZ*(K10M + CX)))
   );
```

```
    CXEqn().relax();
    solve(CXEqn);
    CX = max(CX, 1e-40);
    Info<< "CX min:" << min(CX).value() << endl;
    Info<< "CX max:" << max(CX).value() << endl;
//12
    tmp<fvScalarMatrix> CXaEqn
    (
            fvm::ddt(CXa)
          + fvm::div(phi, CXa)
          - fvm::laplacian(DCXa, CXa)
             - (k10*CVIIIa*CIXa*CX/(KdZ*(K10M + CX)) )
             + fvm::Sp(h10*CATIII,CXa)
             + fvm::Sp(hTFPI*CTFPI,CXa)      //- (k10*CVIIIa*CIXa*CX/(KdZ*(K10M +
CX)) - h10*CXa*CATIII - hTFPI*CTFPI*CXa )
    );
    CXaEqn().relax();
    solve(CXaEqn);
    CXa = max(CXa, 1e-40);
    Info<< "CXa min:" << min(CXa).value() << endl;
    Info<< "CXa max:" << max(CXa).value() << endl;
//13
    tmp<fvScalarMatrix> CXIEqn
    (
            fvm::ddt(CXI)
          + fvm::div(phi, CXI)
          - fvm::laplacian(DCXI, CXI)
             + fvm::Sp((k11)*CIIa/(K11M + CXI) ,CXI)
             + fvm::Sp((k12a)*CXIIa/(K12aM + CXI),CXI)

             //- ((-k11)*CIIa*CXI/(K11M + CXI) + (-k12a)*CXIIa*CXI/(K12aM + CXI)
)
    );
    CXIEqn().relax();
    solve(CXIEqn);
    CXI = max(CXI, 1e-40);
    Info<< "CXI min:" << min(CXI).value() << endl;
    Info<< "CXI max:" << max(CXI).value() << endl;
//14
    tmp<fvScalarMatrix> CXIaEqn
    (
            fvm::ddt(CXIa)
          + fvm::div(phi, CXIa)
          - fvm::laplacian(DCXIa, CXIa)
```

```
            - (k11*CIIa*CXI/(K11M + CXI))
            - (k12a*CXIIa*CXI/(K12aM + CXI))
            + fvm::Sp(h11A3*CATIII,CXIa)
            + fvm::Sp(h11L1*Calpha1AT,CXIa)
            + fvm::Sp(hPCI11a*CCInh,CXIa)

            //- (k11*CIIa*CXI/(K11M + CXI) + k12a*CXIIa*CXI/(K12aM + CXI) -
h11A3*CXIa*CATIII - h11L1*CXIa*Calpha1AT - hPCI11a*CXIa*CCInh)
    );
    CXIaEqn().relax();
    solve(CXIaEqn);
    CXIa = max(CXIa, 1e-40);
    Info<< "CXIa min:" << min(CXIa).value() << endl;
    Info<< "CXIa max:" << max(CXIa).value() << endl;
//15
    tmp<fvScalarMatrix> CPCEqn
    (
          fvm::ddt(CPC)
        + fvm::div(phi, CPC)
        - fvm::laplacian(DCPC, CPC)
            + fvm::Sp((kPC*CIIa/(KPCM + CPC)),CPC)

            //- ((-kPC)*CIIa*CPC/(KPCM + CPC))
    );

    CPCEqn().relax();
    solve(CPCEqn);
    CPC = max(CPC, 1e-40);
    Info<< "CPC min:" << min(CPC).value() << endl;
    Info<< "CPC max:" << max(CPC).value() << endl;

//16
    tmp<fvScalarMatrix> CAPCEqn
    (
          fvm::ddt(CAPC)
        + fvm::div(phi, CAPC)
        - fvm::laplacian(DCAPC, CAPC)
            - (kPC*CIIa*CPC/(KPCM + CPC))
            + fvm::Sp(hPC*Calpha1AT/*/(KPCM + CPC)*/,CAPC)


            //- (kPC*CIIa*CPC/(KPCM + CPC) - hPC*CAPC*Calpha1AT)
    );
```

```
    CAPCEqn().relax();
    solve(CAPCEqn);
    CAPC = max(CAPC, 1e-40);
    Info<< "CAPC min:" << min(CAPC).value() << endl;
    Info<< "CAPC max:" << max(CAPC).value() << endl;
//17
    tmp<fvScalarMatrix> CATIIIEqn
    (
            fvm::ddt(CATIII)
          + fvm::div(phi, CATIII)
          - fvm::laplacian(DCATIII, CATIII)
          + fvm::Sp((h9*CIXa + h10*CXa + h2*CIIa + h11A3*CXIa +
h12A3*CXIIa),CATIII)

             //- ( -(h9*CIXa + h10*CXa + h2*CIIa + h11A3*CXIa +
h12A3*CXIIa)*CATIII   )
    );
    CATIIIEqn().relax();
    solve(CATIIIEqn);
    CATIII = max(CATIII, 1e-40);
    Info<< "CATIII min:" << min(CATIII).value() << endl;
    Info<< "CATIII max:" << max(CATIII).value() << endl;
//18
    tmp<fvScalarMatrix> CTFPIEqn
    (
            fvm::ddt(CTFPI)
          + fvm::div(phi, CTFPI)
          - fvm::laplacian(DCTFPI, CTFPI)
             + fvm::Sp((hTFPI*CXa),CTFPI)

             //- ( -(hTFPI*CTFPI*CXa)   )
    );
    CTFPIEqn().relax();
    solve(CTFPIEqn);
    CTFPI = max(CTFPI, 1e-40);
    Info<< "CTFPI min:" << min(CTFPI).value() << endl;
    Info<< "CTFPI max:" << max(CTFPI).value() << endl;
//19
    tmp<fvScalarMatrix> Calpha1ATEqn
    (
            fvm::ddt(Calpha1AT)
          + fvm::div(phi, Calpha1AT)
          - fvm::laplacian(DCalpha1AT, Calpha1AT)
             + fvm::Sp(hPC*CAPC,Calpha1AT)
```

```
            + fvm::Sp(h11L1*CXIa,Calpha1AT)

            //- ( -hPC*CAPC*Calpha1AT - h11L1*CXIa*Calpha1AT           )
    );
    Calpha1ATEqn().relax();
    solve(Calpha1ATEqn);
    Calpha1AT  = max(Calpha1AT, 1e-40);
    Info<< "Calpha1AT min:" << min(Calpha1AT).value() << endl;
    Info<< "Calpha1AT max:" << max(Calpha1AT).value() << endl;
//20
    tmp<fvScalarMatrix> CtPAEqn
    (
            fvm::ddt(CtPA)
          + fvm::div(phi, CtPA)
          - fvm::laplacian(DCtPA, CtPA)
          //    - (0)
    );
    CtPAEqn().relax();
    solve(CtPAEqn);
    CtPA = max(CtPA, 1e-40);
    Info<< "CtPA min:" << min(CtPA).value() << endl;
    Info<< "CtPA max:" << max(CtPA).value() << endl;
//21
    tmp<fvScalarMatrix> CPLSEqn
    (
            fvm::ddt(CPLS)
          + fvm::div(phi, CPLS)
          - fvm::laplacian(DCPLS, CPLS)
             + fvm::Sp(kPLA*CtPA/(KPLAM + CPLS),CPLS)
             + fvm::Sp(kPLA12a*CXIIa/(KPLA12aM + CPLS) ,CPLS)

             //- (-kPLA*CtPA*CPLS/(KPLAM + CPLS) -
kPLA12a*CXIIa*CPLS/(KPLA12aM + CPLS)   )
    );

    CPLSEqn().relax();
    solve(CPLSEqn);
    CPLS = max(CPLS, 1e-40);
    Info<< "CPLS min:" << min(CPLS).value() << endl;
    Info<< "CPLS max:" << max(CPLS).value() << endl;

//22
    tmp<fvScalarMatrix> CPLAEqn
    (
```

```
          fvm::ddt(CPLA)
        + fvm::div(phi, CPLA)
        - fvm::laplacian(DCPLA, CPLA)
          - (kPLA*CtPA*CPLS/(KPLAM + CPLS))
          - (kPLA12a*CXIIa*CPLS/(KPLA12aM + CPLS))
          + fvm::Sp(hPLA*Calpha2AP,CPLA)

          //- (kPLA*CtPA*CPLS/(KPLAM + CPLS) +
kPLA12a*CXIIa*CPLS/(KPLA12aM + CPLS) - hPLA*CPLA*Calpha2AP  )
   );

   CPLAEqn().relax();
   solve(CPLAEqn);
   CPLA = max(CPLA, 1e-40);
   Info<< "CPLA min:" << min(CPLA).value() << endl;
   Info<< "CPLA max:" << max(CPLA).value() << endl;

//23
   tmp<fvScalarMatrix> Calpha2APEqn
   (
          fvm::ddt(Calpha2AP)
        + fvm::div(phi, Calpha2AP)
        - fvm::laplacian(DCalpha2AP, Calpha2AP)
          + fvm::Sp((hPLA*CPLA + halphaAP*CXIIa),Calpha2AP)


          //- (-(hPLA*CPLA + halphaAP*CXIIa)*Calpha2AP  )
   );

   Calpha2APEqn().relax();
   solve(Calpha2APEqn);
   Calpha2AP = max(Calpha2AP, 1e-40);
   Info<< "Calpha2AP min:" << min(Calpha2AP).value() << endl;
   Info<< "Calpha2AP max:" << max(Calpha2AP).value() << endl;
//24
   tmp<fvScalarMatrix> CXIIEqn
   (
          fvm::ddt(CXII)
        + fvm::div(phi, CXII)
        - fvm::laplacian(DCXII, CXII)
          + fvm::Sp(k12/(K12M + CXII),CXII)
          + fvm::Sp(kkalli*CKalli/(KkalliM + CXII),CXII)

          //- (-k12*CXII/(K12M + CXII) - kkalli*CKalli*CXII/(KkalliM + CXII)   )
```

```
    );
    CXIIEqn().relax();
    solve(CXIIEqn);
    CXII = max(CXII, 1e-40);
    Info<< "CXII min:" << min(CXII).value() << endl;
    Info<< "CXII max:" << max(CXII).value() << endl;
//25
    tmp<fvScalarMatrix> CXIIaEqn
    (
            fvm::ddt(CXIIa)
          + fvm::div(phi, CXIIa)
          - fvm::laplacian(DCXIIa, CXIIa)
             - (k12*CXII/(K12M + CXII))
             - (kkalli*CKalli*CXII/(KkalliM + CXII))
             + fvm::Sp(h12,CXIIa)
             + fvm::Sp(hPCI12a*CCInh,CXIIa)
             + fvm::Sp(halphaAP*Calpha2AP,CXIIa)
             + fvm::Sp(h12A3*CATIII,CXIIa)

              //- (k12*CXII/(K12M + CXII) + kkalli*CKalli*CXII/(KkalliM + CXII) -
h12*CXIIa - hPCI12a*CXIIa*CCInh - halphaAP*CXIIa*Calpha2AP -
h12A3*CXIIa*CATIII  )
    );
    CXIIaEqn().relax();
    solve(CXIIaEqn);
    CXIIa = max(CXIIa, 1e-40);
    Info<< "CXIIa min:" << min(CXIIa).value() << endl;
    Info<< "CXIIa max:" << max(CXIIa).value() << endl;
//26
    tmp<fvScalarMatrix> CCInhEqn
    (
            fvm::ddt(CCInh)
          + fvm::div(phi, CCInh)
          - fvm::laplacian(DCCInh, CCInh)
             + fvm::Sp((hPCI12a*CXIIa + hPCI11a*CXIa),CCInh )

              //- ( -(hPCI12a*CXIIa + hPCI11a*CXIa)*CCInh  )
    );
    CCInhEqn().relax();
    solve(CCInhEqn);
    CCInh = max(CCInh, 1e-40);
    Info<< "CCInh min:" << min(CCInh).value() << endl;
    Info<< "CCInh max:" << max(CCInh).value() << endl;
//27
```

```
    tmp<fvScalarMatrix> CPreKalliEqn
    (
            fvm::ddt(CPreKalli)
          + fvm::div(phi, CPreKalli)
          - fvm::laplacian(DCPreKalli, CPreKalli)
             + fvm::Sp(kPreKA*CXIIa/(KPreKAM + CPreKalli),CPreKalli)
             + fvm::Sp(kPreKB*CXIIa/(KPreKBM + CPreKalli),CPreKalli)

             //- (-kPreKA*CXIIa*CPreKalli/(KPreKAM + CPreKalli) -
kPreKB*CXIIa*CPreKalli/(KPreKBM + CPreKalli)          )
    );
    CPreKalliEqn().relax();
    solve(CPreKalliEqn);
    CPreKalli = max(CPreKalli, 1e-40);
    Info<< "CPreKalli min:" << min(CPreKalli).value() << endl;
    Info<< "CPreKalli max:" << max(CPreKalli).value() << endl;
//28
    tmp<fvScalarMatrix> CKalliEqn
    (
            fvm::ddt(CKalli)
          + fvm::div(phi, CKalli)
          - fvm::laplacian(DCKalli, CKalli)
             - (kPreKA*CXIIa*CPreKalli/(KPreKAM + CPreKalli))
             + fvm::Sp(hkalli,CKalli)


             //- (kPreKA*CXIIa*CPreKalli/(KPreKAM + CPreKalli) +
kPreKB*CXIIa*CPreKalli/(KPreKBM + CPreKalli) - hkalli*CKalli         )
    );
    CKalliEqn().relax();
    solve(CKalliEqn);
    CKalli = max(CKalli, 1e-40);
    Info<< "CKalli min:" << min(CKalli).value() << endl;
    Info<< "CKalli max:" << max(CKalli).value() << endl;
```

VITA

Name: Daniel Edward LaCroix

Address: Non-Linear Mechanics Laboratory
Department of Mechanical Engineering
Texas A&M University, College Station, TX 77843-3123

Education: B.S., Engineering Science, Trinity University, San Antonio, TX (2005)

M.S., Mechanical Engineering, Texas A&M University, College Station, TX (2008)

Ph.D., Mechanical Engineering, Texas A&M University, College Station, TX (2011)

Email: dlacroix21@gmail.com